Simulation of reservoir influences on annual and seasonal streamflow changes for the Lena, Yenisei, and Ob' rivers

Jennifer C. Adam,[1] Ingjerd Haddeland,[2] Fengge Su,[1] and Dennis P. Lettenmaier[1]

Received 9 February 2007; revised 12 July 2007; accepted 19 September 2007; published 28 December 2007.

[1] Since the 1930s, combined streamflow from the largest Eurasian rivers discharging to the Arctic Ocean has been increasing. For many of these rivers, an increase in annual streamflow volume has been accompanied by a shift in seasonality (e.g., earlier snowmelt runoff in the spring). These changes in annual and seasonal streamflow may be due to direct effects of climate change (e.g., increased precipitation, or changes in snow accumulation and ablation patterns), indirect effects of climate change (e.g., changes in permafrost), or human effects (e.g., storage and release of river runoff in reservoirs). We develop and describe a method to estimate the potential contributions of artificial reservoirs to long-term changes in annual and seasonal streamflow between 1937 and 1998. Reservoir effects on downstream flow are simulated using a reservoir routing model coupled off-line to the Variable Infiltration Capacity (VIC) land surface hydrology model for the Lena, Yenisei and Ob' river basins. The effects of reservoirs on basin average evaporation are also represented. We perform trend analysis on long-term (≥30 years) time series of seasonal and annual streamflow and isolate the effects of reservoirs. Although reservoirs have had little effect on trends in annual discharge from the Lena, Yenisei, and Ob' river basins, we conclude that they are responsible for many of the seasonal changes that have been observed. For the Lena, reservoirs account for up to 80% and 30% of the observed winter and spring trends, respectively. For the Yenisei, reservoirs account for up to 100%, 40%, and 60% to 100% of the observed winter, spring, and late summer to early fall trends, respectively. For the Ob', reservoirs may account for more than 70% of the observed trends during the months of January to March. A result of this study is a set of reconstructed streamflow at the outlets of the Lena, Yenisei, and Ob' river basins which can be used in subsequent studies to improve the understanding of climate change effects on runoff generation in the Eurasian Arctic.

Citation: Adam, J. C., I. Haddeland, F. Su, and D. P. Lettenmaier (2007), Simulation of reservoir influences on annual and seasonal streamflow changes for the Lena, Yenisei, and Ob' rivers, *J. Geophys. Res.*, *112*, D2411, doi:10.1029/2007JD008525.

1. Introduction

[2] The climate of the Arctic region has been the focus of extensive recent research partly because observed and predicted warming in the region exceeds the global average. One related concern is that this observed and projected warming has the potential for feedbacks to the global carbon cycle. Another is that related land surface hydrological changes result in feedback responses to global climate through mechanisms related to altered arctic freshwater fluxes [*Arctic Climate Impact Assessment*, 2005]. Streamflow is an effective indicator of hydrologic change because it integrates the effects of climate change spatially over areas up to several million km^2, in the case of the largest Arctic rivers. The three largest Siberian watersheds (the Lena, Yenisei, and Ob') are responsible for more than 45% of the total freshwater discharge into the Arctic Ocean [*Shiklomanov et al.*, 2000]. Therefore analysis of streamflow from these three basins alone can provide insight into how climate has affected and may continue to affect large-scale hydrological processes in the pan-Arctic basin.

[3] In the Eurasian Arctic, increasing annual streamflow volumes and a shift in streamflow seasonality have occurred over the last 70 years [*Berezovskaya et al.*, 2005; *Georgievsky et al.*, 1996; *Lammers et al.*, 2001; *Peterson et al.*, 2002; *Savelieva et al.*, 2000; *Shiklomanov et al.*, 2000, 2006; *Yang et al.*, 2002, 2004a, 2004b; *Ye et al.*, 2003, 2004]. The forces driving these changes are unclear, although numerous factors have been examined, including changes in precipitation, permafrost degradation, changes in snowmelt volume and timing, and enhanced fire frequency [*Adam and Lettenmaier*, 2007; *Berezovskaya et al.*, 2004, 2005; *McClelland et al.*, 2004; *Nijssen et al.*, 2001; *Pavelsky and Smith*, 2006; *Rawlins et al.*, 2006; *Wu et al.*, 2005; *Yang et al.*, 2003; *Ye et al.*, 2004]. A complication is

[1]Department of Civil and Environmental Engineering, University of Washington, Seattle, Washington, USA.
[2]Norwegian Water Resources and Energy Directorate, Oslo, Norway.

0148-0227/07/2007JD008525

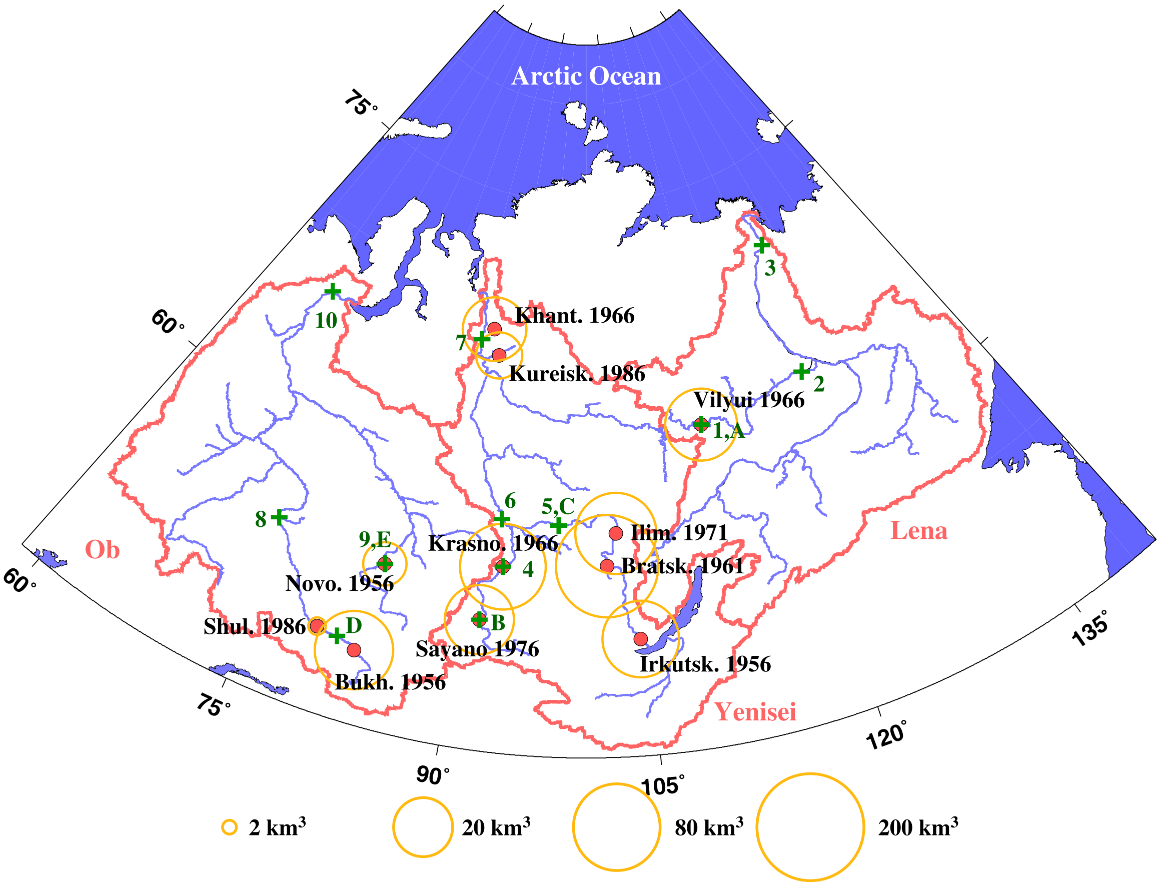

Figure 1. Locations of operational reservoirs for which the storage capacities exceed 1 km^3 (shown as solid red circles) for the Lena, Yenisei, and Ob' river basins (see Table 1 for reservoir characteristics). The storage capacities of the reservoirs are given on a log ten scale by the diameters of the yellow circles. The green pluses indicate the locations of the streamflow gauging stations used either for bias correction of inflow into the farthest upstream reservoir on each tributary (letters A–E, see Table 2 for station information) or for reservoir model evaluation (numerals 1–10, see Table 5 for station information). Some stations are used for both purposes. If a green plus is located directly over a reservoir station, this indicates that the gauging station is just downstream of the reservoir outlet. Note that Boguchanskoe reservoir on the Angara tributary (located at gauging station 5) is not shown because it is not yet operational.

that direct human alterations have also affected streamflow of the major Siberian rivers over the same period [*Berezovskaya et al.*, 2005; *Dynesius and Nilsson*, 1994; *Haddeland et al.*, 2007; *McClelland et al.*, 2004; *Plishkin*, 1979; *Shiklomanov*, 1978; *Shiklomanov and Veretennikova*, 1978; *Shiklomanov et al.*, 2000; *Yang et al.*, 2004a, 2004b; *Ye et al.*, 2003]. For example, the construction and operation of large reservoirs result in a shift in streamflow seasonality which reduces spring and summer peak flows and increases fall and winter low flows. These reservoir-related changes and the shifts in streamflow seasonality resulting from climate change can be confounded, as their effects on streamflow magnitude and timing can be similar [*Georgievsky et al.*, 1996].

[4] Humans can directly affect land surface hydrology by redistributing runoff over space and time, such as by constructing runoff diversions; and by disturbing the natural partitioning of precipitation between runoff, evapotranspiration, and storage changes, such as via reservoir construction, irrigation, or land cover changes [*Shiklomanov*, 1978; *Vörösmarty and Sahagian*, 2000]. Over the Lena, Yenisei, and Ob' river basins, humans have most significantly altered the natural hydrologic regime by the construction and operation of large reservoirs, which have substantially changed streamflow seasonality. For example, *Yang et al.* [2004a] report that two large reservoirs in the upper Yenisei basin have increased winter low flows by 45% to 85% and decreased summer flows by 10% to 50% between 1935 and 1999. Effects on annual streamflow volumes are less significant. Annual consumptive use of water (essentially diversions of water from the river that are not returned) is less than 0.5% [*Berezovskaya et al.*, 2005], between 0.8% and 1.4% [*Shiklomanov et al.*, 2000], and less than 1% [*Dynesius and Nilsson*, 1994] of the mean annual flow at the outlets of the Lena, Yenisei, and Ob' river basins, respectively. Increases in annual evaporation due to reservoir construction are of similar magnitude: up to 0.1%, 0.1% to 0.5%, and 0.6% to 1.0% of the mean annual flow

Table 1. Characteristics of the Large (>1 km^3) Operational Reservoirs in the Lena, Yenisei, and Ob' River Basins[a]

Reservoir	Tributary	Basin	First Year of Filling	Capacity, km^3	Fraction of Annual Inflow	Fraction of Annual Flow at Basin Outlet	Surface Area, km^2	Dam Height, m	f	f'
Vilyuiskoe	Vilyui	Lena	1966	35.9	1.77	0.07	2170	64	1327	906
Sayano-Shushenskoe	Yenisei	Yenisei	1976	31.3	0.65	0.05	621	245	233	113
Krasnoyarskoe	Yenisei	Yenisei	1966	73.3	0.81	0.13	2000	124	575	480
Irkutskoe[b]	Angara	Yenisei	1956	46/23680	0.78/402.71	0.08/40.79	3300/34794	44	1943/129	1800/164
Bratskoe	Angara	Yenisei	1961	169	1.90	0.29	5470	125	1128	721
Ust'-Ilimskoe	Angara	Yenisei	1971	59.3	0.54	0.10	1890	102	653	579
Kureiskoe	Kureika	Yenisei	1986	9.9	not gauged	0.02	500	81	532	334
Ust'-Khantaiskoe	Khantaika	Yenisei	1966	23.5	2.66	0.04[c]	2120	65	1958	717
Bukhtarminskoe	Irtish	Ob'	1956	49.8	5.28	0.13	5490	90	3851	640
Shul'binskoe	Irtish	Ob'	1986	2.4	0.08	0.01	255	36	800	556
Novosibirskoe	Ob'	Ob'	1956	8.8	0.15	0.02	1070	27	1875	1638

[a]Information is obtained from *ICOLD* [2003], *Malik et al.* [2000], *McClelland et al.* [2004], and *Vörösmarty et al.* [1997]. Fraction of annual inflow is calculated by dividing the reservoir storage capacity by the average annual flow of the nearest gauging station using the R-ArcticNET data set [*Lammers and Shiklomanov*, 2000]. Fraction of annual flow at basin outlet is calculated by dividing the reservoir storage capacity by the average annual flow at the most downstream station in each of the Lena, Yenisei, and Ob' river basins (stations 3, 7, and 10, respectively, in Table 5). The ratio of the characteristic length to the depth of the reservoir, *f*, is calculated according to equation (2). The alternate value is *f'* and is calculated using equation (4).

[b]The Irkutskoe reservoir is conjoined to Lake Baikal, a natural lake [*Vyruchalkina*, 2004]. The values before the slashes in this row describe the Irkutskoe reservoir were it separate from Lake Baikal, whereas the values after the slash describe the combined Irkutskoe/Baikal system. The smaller volume, 46 km^3, is the regulated capacity of the system (see section 2.2.3.4), whereas the combine dimensions are used to describe the shape of the system (see section 2.2.3.3).

[c]The confluence of the Khantaika tributary and the Yenisei River is downstream of the Igarka gauging station (station 7 in Table 5); therefore the effects of this reservoir are not seen in the streamflow at the Yenisei basin outlet.

for the Lena, Yenisei, and Ob' river basins, respectively (S. Berezovskaya et al., On long-term runoff variability of the largest Siberian rivers, manuscript in preparation, 2007, hereinafter referred to as Berezovskaya et al., manuscript in preparation, 2007). Two other effects on annual streamflow volume occur after reservoir construction. Filling of the reservoir and increase in groundwater storage due to the raising of the water table in the areas surrounding the reservoir can take up to 8 years after reservoir construction (Berezovskaya et al., manuscript in preparation, 2007). Interbasin water diversions are another means by which the seasonality and annual volumes of streamflow can be altered, but in the three Siberian rivers in question, these effects are small. Diversions into the Ob' River basin amount to 0.5% of its mean annual flow, while diversions are negligible in the other two basins [*Dynesius and Nilsson*, 1994].

[5] The goal of this study is to isolate the effects of the reservoirs on long-term ($\geq$30 years) annual and seasonal streamflow trends between 1937 and 1998 from other causes. We apply a coupled hydrology-routing-reservoir model to simulate the effects of reservoirs on streamflow. As a result of these analyses, we produce reconstructed streamflow time series, in which the primary effects of reservoirs have been removed from streamflow at the outlets of the Lena, Yenisei, and Ob' river basins. Our analyses account for the shift in streamflow seasonality due to reservoir operations, and the effects of reservoir evaporation and filling on annual streamflow volume. We do not account for the other effects on annual streamflow volume, although these effects, with exception of the small diversion of water into the Ob' River basin, result in a decrease in volume, and therefore cannot explain observed streamflow increases. We compare our reconstructed product to those developed using only streamflow observations [*McClelland et al.*, 2004; *Yang et al.*, 2004a; *Ye et al.*, 2003]. The unique contribution of this work is that it uses a physically based representation of reservoir operations to provide an estimate of the potential effects that reservoirs have had on Eurasian Arctic streamflow. This paper is one of a three-part study to improve our understanding of the causes of observed streamflow changes in northern Eurasia. The other two papers perform trend analysis on precipitation, temperature, and observed and reconstructed streamflow to identify basins for which precipitation changes can account for historical streamflow changes [*Adam and Lettenmaier*, 2007] and evaluate the sensitivity of simulated streamflow to precipitation and temperature changes (J. C. Adam and D. P. Lettenmaier, Application of a macroscale hydrologic model to a streamflow trend attribution study in northern Eurasia, manuscript in preparation, 2007, hereinafter referred to as Adam and Lettenmaier, manuscript in preparation, 2007).

2. Methods

2.1. Selection of Reservoirs for Analysis

[6] Eleven large reservoirs were constructed in the Lena, Yenisei, and Ob' river basins between 1950 and 1990, four of which are among the ten largest hydroelectric facilities in the world [*International Commission on Large Dams*

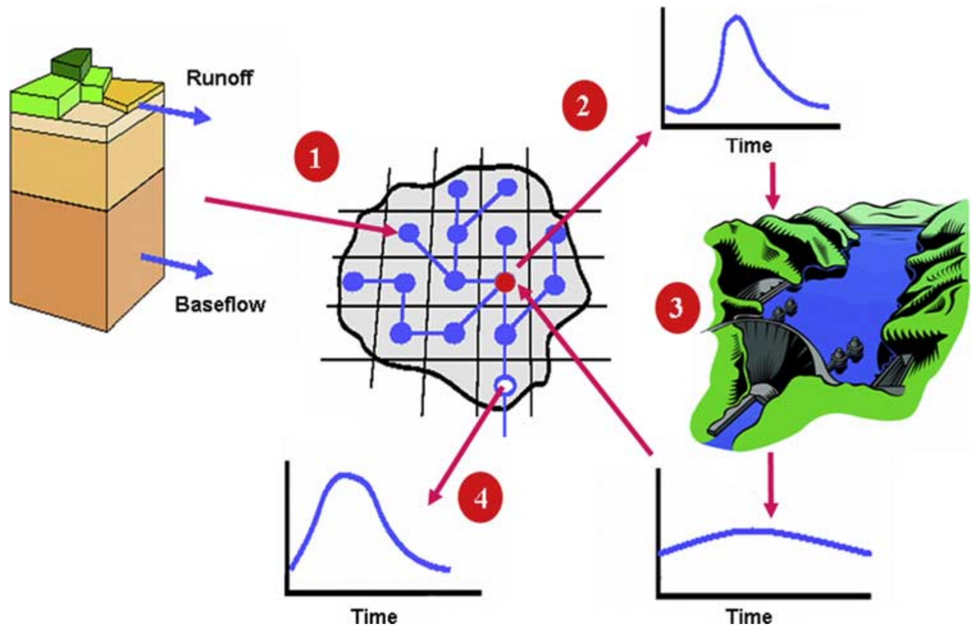

Figure 2. Coupling schematic for (1) hydrology [*Cherkauer and Lettenmaier*, 1999; *Liang et al.*, 1994; *Su et al.*, 2005; Adam and Lettenmaier, manuscript in preparation, 2007], (2) routing [*Lohmann et al.*, 1996, 1998], and (3) reservoir [*Haddeland et al.*, 2006a, 2006b, 2007] models.

(*ICOLD*), 2003]. The locations and some characteristics of these reservoirs are given in Figure 1 and Table 1, respectively. Other reservoirs were not included in this analysis for various reasons. The Boguchansky reservoir (on the Angara River) was not considered because it is not yet operational. Furthermore, ''small'' reservoirs (with storage capacities less than 1 km^3) were excluded. For example, we did not analyze the Ust'-Kamengorsky reservoir on the Irtish River because it has a reservoir capacity of only 0.6 km^3, and *Yang et al.* [2004b] did not detect effects of this reservoir on downstream discharge. A small reservoir on the Vitim River in the Lena River basin was excluded for the same reason [*Berezovskaya et al.*, 2005].

2.2. Modeling Framework

[7] We used a hydrology/routing/reservoir coupled model system, as shown in Figure 2. The steps involved in the process are as follows:

[8] 1. Run the grid-based hydrology model (driven with observed precipitation, temperature, and other surface meteorological variables; see section 2.2.1 and *Nijssen et al.* [1997] for details) for each grid cell and combine the simulated runoff and base flow as input to the routing model.

[9] 2. For all grid cells upstream of the reservoir, route the runoff to the reservoir (red cell in Figure 2) and bias correct the simulated streamflow using prereservoir observed streamflow data. The bias correction procedure is described in section 2.2.2.

[10] 3. Run the reservoir model for each operational year by maximizing revenue from hydropower production. The reservoir model is described in section 2.2.3.

[11] 4. Route reservoir releases and all other basin contributions to the basin outlet.

2.2.1. Hydrology and Routing Models

[12] We used the Variable Infiltration Capacity (VIC) large-scale hydrology model [*Liang et al.*, 1994; *Nijssen et al.*, 1997]. The version we used includes algorithms that are important for processes occurring in northern Eurasia [*Cherkauer et al.*, 2003]: a lakes and wetlands model [*Bowling*, 2002], an algorithm for the sublimation and redistribution of blowing snow [*Bowling et al.*, 2004], a

Table 2. Streamflow Gauging Stations (From the R-ArcticNET Data Set [*Lammers and Shiklomanov*, 2000]) Used for Bias Correction of Inflow to the Farthest Upstream Reservoir in Each Tributary[a]

Reservoir	Tributary	Basin	Streamflow Gauging Station	ID	Period
Vilyuiskoe	Vilyui	Lena	Vilyui at Chernyshevskiy	A	1959–1965
Sayano-Shushenskoe	Yenisei	Yenisei	Yenisei at Nikitino	B	1931–1975
Irkutskoe	Angara	Yenisei	Angara at Boguchany	C	1936–1955
Bukhtarminskoe	Irtish	Ob'	Irtish at Shul'ba	D	1937–1955
Novosibirskoe	Ob'	Ob'	Ob at Novosibirsk	E	1936–1955

[a]Bias correction was not performed for the Kureiskoe reservoir because of the lack of observed streamflow data for this tributary, or the Ust'-Khantaiskoe reservoir because the Khantaika tributary discharges to the Yenisei River downstream of the Igarka gauging station. The location of each station is shown in Figure 1 according to the station ID (A through E).

Table 3. Minimum Flow Released From Each Reservoir Calculated as the Mean of Winter (DJF) Flow for the Record Period After Reservoir Construction[a]

Reservoir	Streamflow Gauging Station	Minimum Qr, $m^3\ s^{-1}$
Vilyuiskoe	Vilyui at Chernyshevskiy (ID = 1)	738
Sayano-Shushenskoe	Yenisei at Nikitino (ID = B)	986
Krasnoyarskoe	Yenisei at Krysnoyarskaya GES	2819
Irkutskoe	Angara at Irkutskaya GES	1868
Bratskoe	Angara at Bratskaya GES	3074
Ust'-Ilimskoe	Angara at Boguchany (ID = 5)	3282
Kureiskoe	7Q10 of Naturalized Flow	232
Ust'-Khantaiskoe	7Q10 of Naturalized Flow	26
Bukhtarminskoe	Irtish at Shul'ba	468
Shul'binskoe	Irtish at Omsk (ID = 8)	523
Novosibirskoe	Ob' at HPS Novosibirskaya	612

[a]The nearest downstream streamflow gauging station (from the R-ArcticNET data set [*Lammers and Shiklomanov*, 2000]) to each reservoir was selected for the calculation. For reservoirs with no nearby downstream gauging station, the 7-d consecutive low flow with a 10-year recurrence period (7Q10) was calculated from the naturalized simulated streamflow at the reservoir location (following *Haddeland et al.* [2006a, 2006b, 2007]). Note that for gauging stations identified with names other than that of the upstream reservoir, the station IDs (corresponding to the locations shown in Figure 1) are given.

finite difference frozen soils algorithm [*Cherkauer and Lettenmaier*, 1999] with subgrid frost variability [*Cherkauer and Lettenmaier*, 2003], and a two-layer energy balance snow model [*Storck and Lettenmaier*, 1999] that allows for subgrid variability in snow cover [*Cherkauer and Lettenmaier*, 2003]. We used the *Su et al.* [2005] pan-Arctic implementation of the VIC model at an Equal-Area Scalable Earth Grid (EASE-Grid) [*Brodzik*, 1997] spatial resolution of approximately 100 km. *Su et al.* [2005] describe the data involved in creating this setup, the calibration of soil depths and infiltration characteristics using observed streamflow data for a constrained period (1979 to 1999), and the evaluation of the simulations using observed snow cover extent, lake freezeup and breakup dates, and permafrost active layer thickness. We ran the model in full energy mode (in which the model iteratively solves the effective surface temperature by resolving the energy and water balances) at a 3-hourly time step from 1930 to 2000. There are three differences between the *Su et al.* [2005] implementation and this implementation: (1) a longer simulation period (*Su et al.* [2005] used the period from 1979 to 1999), (2) forcing data, and (3) modifications to the frozen soils algorithm, of which the latter two are discussed briefly below.

[13] The VIC model is forced with daily gridded precipitation, maximum and minimum temperature, and wind speed, which are downscaled to the model time step of three hours using methods described by *Maurer et al.* [2002]. From these data, vapor pressure, incoming shortwave radiation, and net long-wave radiation are calculated using algorithms described by *Maurer et al.* [2002]. Monthly time series of gridded precipitation and temperature are based on meteorological station observations for which we used the products of *Willmott and Matsuura* [2005] and *Mitchell and Jones* [2005], respectively. To improve the monthly precipitation estimates, we applied the *Adam and Lettenmaier* [2003] corrections for the undercatch of solid and liquid precipitation in manual gauges and the *Adam et al.* [2006] corrections for orographic effects on the interpolation of precipitation point measurements over mountainous regions. Furthermore, we made adjustments for spurious trends in the monthly precipitation product using the method of *Hamlet and Lettenmaier* [2005]. For this, we used a set of high-quality precipitation station data with long-term records [from *Groisman*, 2005] to constrain the low-frequency variability of the original gridded product [*Willmott and Matsuura*, 2005], which was derived from a much denser network of stations. These adjustments are intended to avoid trends that are artifacts of changing

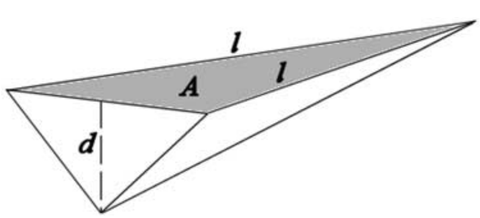

Figure 3. Theoretical shape used for the reservoir storage-area-depth relationships. Reprinted from *Liebe et al.* [2005] with permission from Elsevier.

Table 4. Calibration Parameters, *Cv* and *Ns*, for the Monthly Pricing Distribution Determined by Minimizing the Differences Between Observed and Simulated Reservoir Signatures at the Locations of the Gauging Stations Listed in Column 2[a]

Reservoir	Streamflow Gauging Station	Cv	Ns
Vilyuiskoe	Vilyui at Chernyshevskiy (ID = 1)	0.7	5
Sayano-Shushenskoe	Yenisei at Bazaikha (ID = 4)	0.36	3
Krasnoyarskoe	Yenisei at Bazaikha (ID = 4)	0.36	3
Irkutskoe	Angara at Boguchany (ID = 5)	0.46	12
Bratskoe	Angara at Boguchany (ID = 5)	0.46	12
Ust'-Ilimskoe	Angara at Boguchany (ID = 5)	0.46	12
Kureiskoe	Angara at Boguchany (ID = 5)[b]	0.46	12
Ust'-Khantaiskoe	Angara at Boguchany (ID = 5)[b]	0.46	12
Bukhtarminskoe	Irtish at Omsk (ID = 8)	0.44	5
Shul'binskoe	Irtish at Omsk (ID = 8)	0.44	5
Novosibirskoe	Ob at Novosibirsk (ID = 9)	0.1	3

[a]Reservoirs sharing the same selected gauging station were calibrated simultaneously and therefore have the same calibrated values. Note that the station IDs (corresponding to the locations shown in Figure 1) are given in parentheses.

[b]Streamflow observations were not available downstream of the Kureiskoe and Ust'-Khantaiskoe reservoirs, therefore they were given the same values as the Angara reservoirs.

Table 5. Streamflow Gauging Stations (From the R-ArcticNET Data Set [*Lammers and Shiklomanov*, 2000]) Used for Evaluation of the Simulated Reservoir Signature on Mean Monthly Streamflow[a]

ID	Streamflow Gauging Station	Basin	Period of Record	Contributing Area, km^2	Upstream Large Reservoirs	Prereservoir Period	Postreservoir Period
1	Vilyui at Chernyshevskiy	Lena	1959–1994	140000	1	1959–1966	1970–1994
2	Vilyui at Khatyrik-Khomo	Lena	1936–1998	450000	1	1936–1966	1970–1998
3	Lena at Kusur	Lena	1934–2000	2430000	1	1936–1966	1970–1999
4	Yenisei at Bazaikha	Yenisei	1902–1999	300000	2	1936–1966	1980–1999
5	Angara at Boguchany	Yenisei	1936–1999	870000	3	1936–1956	1975–1999
6	Yenisei at Yeniseisk	Yenisei	1936–1999	1400000	5	1936–1956	1980–1999
7	Yenisei at Igarka	Yenisei	1936–1999	2440000	6	1936–1956	1980–1999
8	Irtish at Omsk	Ob'	1936–1999	770000	2	1936–1956	1990–1999
9a	Ob at Novosibirsk	Ob'	1936–1962	250000	1	1936–1956	NA
9b	Ob at HPS Novosibirskaya	Ob'	1958–2000	230000	1	NA	1960–1999
10	Ob' at Salekhard	Ob'	1930–1999	2950000	3	1936–1956	1990–1999

[a]The location of each station is shown in Figure 1 according to the station ID (1 through 10).

networks; instead, decadal (and longer) variability in gridded precipitation reflects observed changes in a set of long-term stations. This procedure is described in detail by *Adam and Lettenmaier* [2007]. Daily disaggregation was achieved by rescaling daily NCEP/NCAR reanalysis data [*Kalnay et al.*, 1996] to match the observation-based monthly time series of precipitation and temperature. For this we used the product of *Sheffield et al.* [2004] which includes rainy day bias corrections. For wind speed, daily NCEP/NCAR reanalysis data [*Kalnay et al.*, 1996] were used without rescaling. Prior to 1948, daily disaggregation was performed using a method described by *Wood et al.* [2004] in which monthlong daily patterns of precipitation, temperature, and wind speed were sampled at random from the 1948 to 2000 period of existing daily reanalysis data.

[14] We made three major modifications to the VIC model algorithms for simulation of frozen soils in permafrost regions.

[15] 1. *Su et al.* [2005] experienced problems with the parameterization of frozen soils in Arctic regions, particularly with respect to the soil column bottom boundary. As suggested by *Cherkauer et al.* [2003], rather than treating the lower boundary as constant-temperature, we treat it as zero-flux. This allows for a dynamic bottom boundary temperature which can be predicted as a function of climatic, soil, and ground cover (including vegetation and snow) conditions. This change necessitates increasing the lower boundary depth to at least three times the annual temperature damping depth [*Sun and Zhang*, 2004], in our case from 4 to 15 m. Temperature at the bottom boundary was initialized using gridded observed soil temperature data [*Frauenfeld et al.*, 2004], and we spun up soil column temperature and moisture by running the model for 60 years using forcing data constrained to the climate of the 1930s.

[16] 2. Rather than solve the heat equation explicitly for each node, we solved for all the soil temperatures and ice contents simultaneously using the implicit Newton-Raphson method [*Press et al.*, 1992]. This method is unconditionally stable and also decreases simulation time.

[17] 3. Because the greatest variability in temperature occurs at the near surface thermal nodes, we distributed the nodes exponentially with depth. We used 18 thermal nodes in a soil column of 15 m which results in node spacings of 20 cm near the surface and 2.5 m near the bottom boundary. We performed a grid transformation in which the physical system exists in exponential space, while the heat equations are solved in linear space.

[18] The *Lohmann et al.* [1996, 1998] routing model is coupled off-line to the VIC hydrology model. The routing model transports the combined surface runoff and base flow to the outlet of any grid cell of interest in the basin. The Unit Hydrograph approach is used for within-cell routing, and the linearized Saint-Venant equations are used for channel routing. The model assumes that all runoff exits a cell in a single flow direction (of which there are eight possible directions) and uses the convolution integral to calculate accumulated flux.

2.2.2. Bias Correction

[19] Because the seasonality of inflow to the reservoir strongly affects the storage and release of water from the reservoir, we corrected the streamflow bias at the inlet of the farthest upstream reservoir for each tributary. We applied the probability-mapping technique of *Snover et al.* [2003] in which percentile maps are generated for each calendar month for both observed and simulated streamflow populations for the period of overlap. For each month in the simulated time series, the percentile for the simulated value was identified relative to the empirical probability distribution of observed flows for that month. The bias corrected value is then equal to the observed discharge corresponding to this percentile. (For additional information, see http://www.hydro.washington.edu/Lettenmaier/permanent_archive/hamleaf/bams_paper/technical_documentation.pdf.) To preserve the effects of reservoirs that operate in series along a single tributary, we did not bias correct streamflow at the inlets of reservoirs that are downstream of other reservoirs. Therefore the runoff contributions that enter the river network between reservoirs are not bias-corrected, although these contributions to downstream discharge are less than the headwater contributions. The streamflow gauging

Table 6. RMSE Values Between Simulated and SWMSA Stage Height, Averaged for Each Season[a]

Season	Lake Baikal	Bratskoe Reservoir	Mean
DJF	0.07	1.83	0.95
MAM	0.24	1.63	0.94
JJA	0.22	1.87	1.05
SON	0.20	1.73	0.97

[a]Units are in m.

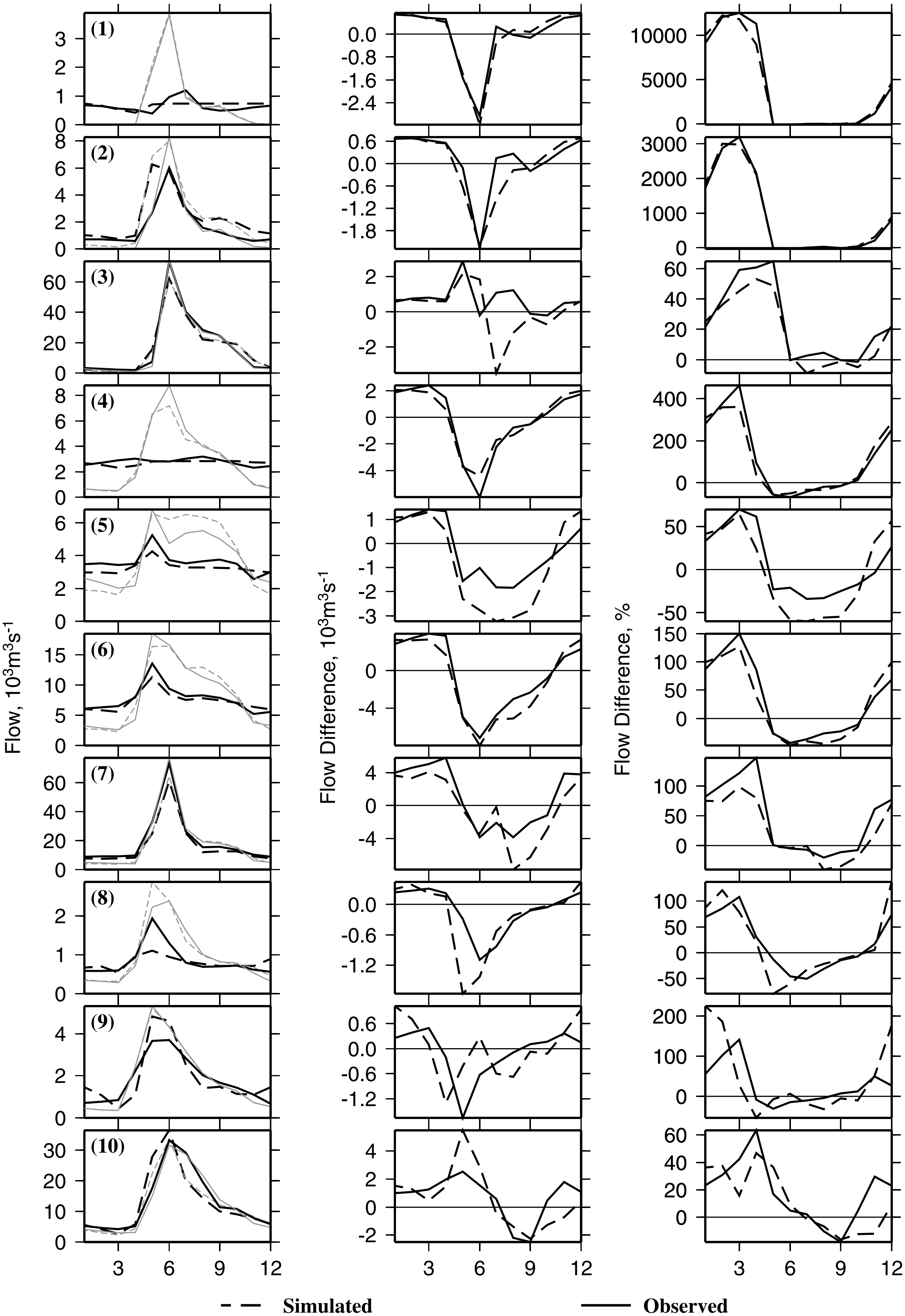

(1)
(2)
(3)
(4)
(5)
(6)
(7)
(8)
(9)
(10)
Flow, $10^3 m^3 s^{-1}$
Flow Difference, $10^3 m^3 s^{-1}$
Flow Difference, %
3
6
9
12
Simulated
Observed

Figure 4

Table 7. Comparison of Observed and Simulated Mean Annual Streamflow at Each of the Evaluation Gauging Stations[a]

	Before, 10^3 m^3 s^{-1}		After, 10^3 m^3 s^{-1}		Difference, 10^3 m^3 s^{-1}		% Difference	
ID	Observed	Simulated	Observed	Simulated	Observed	Simulated	Observed	Simulated
1	0.70	0.73	0.65	0.69	−0.05	−0.04	−6.94	−6.38
2	1.48	2.26	1.62	2.28	0.13	0.02	9.01	1.37
3	16.27	16.21	17.04	16.39	0.77	0.18	4.76	1.10
4	2.93	2.78	2.78	2.70	−0.15	−0.08	−5.28	−2.64
5	3.80	4.02	3.57	3.26	−0.23	−0.76	−6.02	−19.93
6	8.12	8.25	7.65	7.30	−0.47	−0.95	−5.82	−11.72
7	18.29	16.61	19.49	16.44	1.19	−0.17	6.52	−0.91
8	0.95	1.01	0.83	0.80	−0.11	−0.21	−11.79	−22.41
9	1.88	1.87	1.80	1.89	−0.08	0.02	−4.49	0.91
10	12.15	11.84	12.86	12.46	0.71	0.62	5.87	5.10

[a]The station IDs correspond to those in Figure 1 and Table 5. Columns 2 and 3 are prereservoir streamflow at reservoir outlet. Columns 4 and 5 are postreservoir streamflow at reservoir outlet. Columns 6 and 7 are the difference between postreservoir and prereservoir mean annual streamflow. Columns 8 and 9 are percent difference (with respect to observed prereservoir mean annual flow) between postreservoir and prereservoir mean annual streamflow.

stations nearest to each of the farthest upstream reservoirs were selected for bias correction. If the gauging station was downstream of the reservoir, the period of observation record before dam construction was used for bias correction training. Table 2 lists the selected stations for five of the regulated tributaries, which are indicated by letters A through E in Figure 1.

2.2.3. Reservoir Model

[20] We applied the *Haddeland et al.* [2006a, 2006b, 2007] reservoir model which is intended to be used for large-scale modeling in regions where reservoir management details (i.e., operating policies) are not available. For hydroelectric dams, the reservoir model operates by maximizing hydropower production for each operational year using an optimization scheme based on the SCEM-UA algorithm [*Vrugt et al.*, 2003]. While this approach of maximizing hydropower for a single operational year is not completely applicable to reservoirs that are regulated on a multiannual basis such as the Bratskoe reservoir [*Korobova*, 1968], this relatively simple reservoir operations model nonetheless should give us an understanding of the effects of the reservoirs on long-term trends (≥30 years), over which time period the differences between single-year and multiannual operations are somewhat muted. The operational year is identified for each reservoir and begins in the month when the mean monthly simulated naturalized streamflow rate shifts to being less than the mean annual streamflow rate (following *Hanasaki et al.* [2006]). The reservoir model is operated at a daily time step and determines reservoir releases, storage, and evaporation. Reservoir evaporation is calculated using the Penman equation for potential evaporation, which is subtracted from reservoir storage each day. To maintain a reservoir water balance, daily precipitation is added to the reservoir surface. To improve parameterization of the model in the Siberian basins, we made several modifications to the *Haddeland et al.* [2006a, 2006b, 2007] setup as follows.

2.2.3.1. Estimation of Minimum Allowable Reservoir Outflow

[21] To estimate the minimum release from each reservoir, *Haddeland et al.* [2006a, 2006b, 2007] use *7Q10*, the 7-d 10-years recurrence interval low flow, which is calculated from naturalized simulated streamflow at each reservoir location. Because long-term observation records exist downstream of most of the reservoirs in these basins, we instead set the minimum flow to the mean of winter (DJF) observed streamflow after reservoir construction (Table 3). For reservoirs with insufficient nearby streamflow data, we apply *7Q10*.

2.2.3.2. Reservoir Filling

[22] Because we use the reservoir simulation results for long-term trend studies, we needed to allow for reservoirs to come online at the end of the construction period. This is followed by a period of reservoir filling. The years filling began are shown in Table 1. During the filling period, reservoir discharge is maintained at minimum flow (Table 3) and the remainder of the inflow to the reservoir is used for reservoir filling until the reservoir reaches capacity. This results in a filling period of 2 to 5 years.

2.2.3.3. Reservoir Storage-Area-Depth Relationships

[23] Whereas the original *Haddeland et al.* [2006a, 2006b, 2007] system uses a rectangular reservoir shape (vertical walls), we apply the *Liebe et al.* [2005] formulation. This shape is described by a top-down square-based pyramid that has been cut in half (Figure 3). The volume of this shape is given by

$$V = \frac{1}{3} \cdot A \cdot d \ , \qquad (1)$$

where the area of the base of the half pyramid, A, is given by $^1\!/_2 \cdot l^2$, and the height of the pyramid, d, is given by l/f, in which l is the characteristic length of the reservoir. Using

Figure 4. Comparison of observed and simulated monthly reservoir signatures at each of the evaluation gauging stations. The station IDs correspond to those in Figure 1 and Table 5. (left) Prereservoir (thin lines) and postreservoir (bold lines) streamflow at reservoir outlet. (middle) Difference between postreservoir and prereservoir mean monthly streamflow. (right) Percent difference (with respect to observed prereservoir mean monthly flow) between postreservoir and prereservoir mean monthly streamflow.

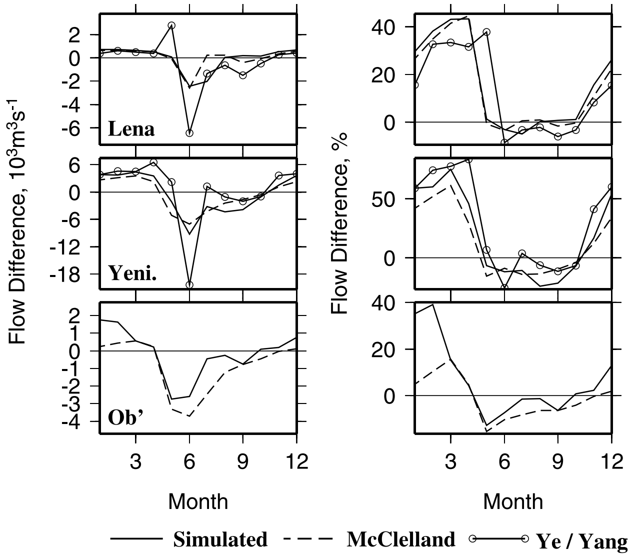

Figure 5. Comparison of simulated monthly reservoir signatures to the reservoir signatures inferred from three reconstructed streamflow products (*McClelland et al.* [2004]; for the Lena, *Ye et al.* [2003]; and for the Yenisei, *Yang et al.* [2004a]) at the outlets of the Lena, Yenisei, and Ob' river basins (gauging stations 3, 7, and 10, respectively; see Figure 1 and Table 5).

these relationships, the dimensionless constant, *f*, can be determined as

$$f = \frac{\sqrt{2}}{3} \cdot \frac{A_{\max}^{3/2}}{V_{\max}}. \quad (2)$$

We estimate *f* for each reservoir from maximum storage and surface area information (Table 1). This allows us to calculate both surface area and depth as a function of storage according to equations (3) and (4).

$$A = \left(\frac{3 \cdot f \cdot V}{\sqrt{2}}\right)^{2/3} \quad (3)$$

$$d = \left(\frac{6 \cdot V}{f^2}\right)^{1/3} \quad (4)$$

Allowing surface area to vary with volume improves the estimation of reservoir evaporation. We use reservoir depth as a proxy for hydrostatic head, *h*. This formulation provides an improvement to the optimization process because it more realistically simulates the slow change in head with storage when the reservoir is full, and a faster change in head with storage when the reservoir is less full. Note that an alternate value of *f*, which we denote as f', can be calculated by rearranging equation (4) (i.e., f' = sqrt(6 $\cdot$ $V_{\max}/d_{\max}^3$), where $d_{\max}$ is the dam height), assuming that the dam height is representative of the reservoir depth near the dam when the reservoir is at capacity. Comparing *f* to f' (see Table 1) gives a rough indication as to how well this theoretical shape describes the relationships between *V*, *A*, and *d*. With the exception of the Bukhtarminskoe reservoir, which has a relatively large surface area with respect to its storage capacity, and to a lesser extent the Sayano-Shushenskoe and Ust'-Khantaiskoe reservoirs, *f* and f' are of comparable magnitude.

2.2.3.4. Minimum Storage

[24] When values of active or regulated storage could be found in the literature, we added an additional constraint on minimum storage, which was calculated as storage capacity minus active storage. Active storage values were found for the Irkutskoe/Baikal system (46 km^3 [*Vyruchalkina*, 2004]), the Bratskoe reservoir (48.2 km^3 [*Nazarov*, 1985]), and the Ust'-Ilimskoe reservoir (2.8 km^3 [*Vyruchalkina*, 2004]). For the Sayano-Shushenskoe reservoir, active storage was calculated using equation (4) and f', given that the top of dead storage is 42 m below the top of the dam [*Stafievskii et al.*, 2003]). This resulted in a value of 13.5 km^3.

2.2.3.5. Maximization of Hydropower Revenue

[25] *Haddeland et al.* [2007] suggest that the reservoir simulations may be improved in Arctic regions if the seasonal variability of the economic value of hydropower is considered. Doing so results in the inclusion of the variable *P* (the monthly varying price of hydropower) in the following objective function:

$$\min \sum_{i=1}^{Ndays} \frac{1}{P \cdot Q_i \cdot \eta \cdot \rho \cdot g \cdot h_i}, \quad (5)$$

where *i* is day of year, *Ndays* is the number of days in the year, *Q* is reservoir release, ρ is the density of water, η is the efficiency of the power generating system, *h* is the hydrostatic head, and *g* is the acceleration due to gravity. Note that this objective function produces identical results to the original *Haddeland et al.* [2006a, 2006b, 2007] formulation if *P* is constant; that is, the monthly pricing coefficient of variation is zero. Because historical hydropower demands are unknown, we use the monthly pricing curve as a means to calibrate the monthly signature of each reservoir on streamflow. This method is therefore a surrogate to reproduce historical reservoir operations given the different purposes for the hydropower produced at each reservoir. We perform the following steps:

[26] 1. We use a sine curve for the pricing distribution, as follows:

$$P_m = P\text{mean} \cdot \left\{\frac{Cv}{0.71}\left[\sin\left(\frac{\Pi}{6}(m + Ns)\right)\right] + 1\right\}, \text{ for } m = 1:12 \quad (6)$$

in which P_m is the price of hydropower for month *m*, *P*mean is the mean annual or base hydropower price, *Cv* is the coefficient of variation of the distribution, and *Ns* is the phase shift of the function. *Cv* and *Ns* are the two calibration parameters. Note that the value 0.71 is the coefficient of variation of the function sin(Π/6(*m* + *Ns*)).

[27] 2. The average cost of hydropower in the Soviet Union in 1990 was 0.15 kopecks per kWh [*Platov*, 1995], and we use this value as our mean annual price in hydropower, *Pmean*.

[28] 3. We calibrated for the values of *Cv* and *Ns* by minimizing the difference between the simulated and observed "reservoir signatures" at gauging stations down-

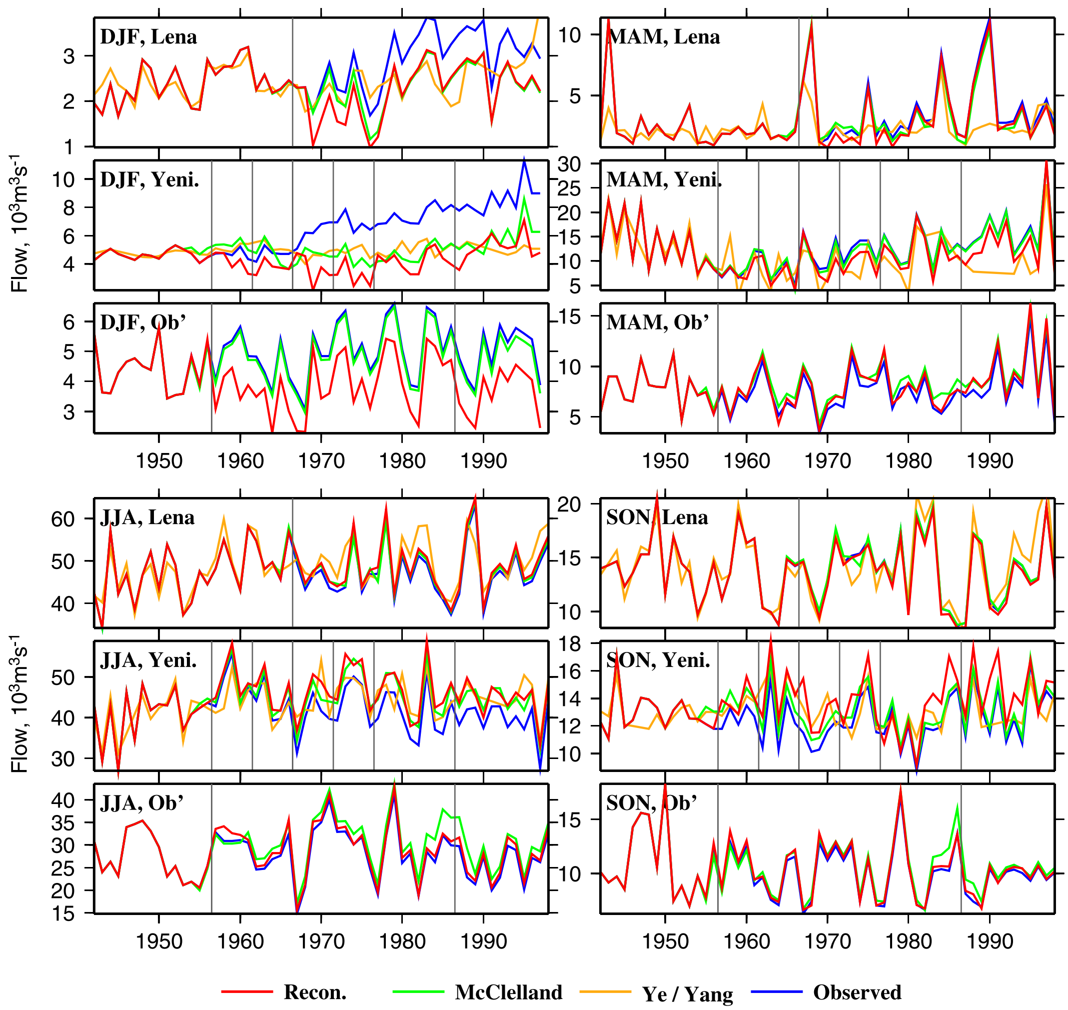

Figure 6. Comparison of seasonal flows for four reconstructed streamflow products (ours; *McClelland et al.* [2004]; for the Lena, *Ye et al.* [2003]; and for the Yenisei, *Yang et al.* [2004a]) to observed streamflow at the outlets of the Lena, Yenisei, and Ob' river basins. Note that DJF is winter, MAM is spring, JJA is summer, and SON is fall. Vertical gray lines indicate the year when filling began for each reservoir in the basin.

stream of the reservoirs. Reservoir signature is defined as the change in the mean monthly hydrograph as a result of reservoir operations. The assumption here is that these changes are entirely due to reservoir operations, although in reality some of these changes may be attributable to other effects (e.g., climate change). The key difference between reservoir and climate influences is that the reservoirs should cause an abrupt change in streamflow during the reservoir filling period and immediately thereafter, whereas climate influences should result in more gradual changes. Therefore the gradual effects of climate will still be apparent in the trend results shown in section 3.3. *Cv* was constrained to values between 0 and 0.7 (because values greater than 0.7 caused the prices to become negative in some months) and *Ns* was constrained to values between 1 and 12. The values are given in Table 4. See section 3.1 for results.

2.3. Development of the Reconstructed Product

[29] We created a reconstructed streamflow product which accounts for the effects of reservoirs as follows. The coupled modeling system was run with and without the reservoir model. At each of the downstream-most gauging stations in the three basins (stations 3, 7, and 10 in Figure 1 and Table 5) we subtracted the naturalized routed streamflow from the routed streamflow with reservoir effects. These values were then subtracted from observed streamflow. This procedure effectively cancels out the biases that exist in simulated streamflow. Also, before the reservoirs come online, the reconstructed product is identical to observed streamflow. Comparisons of this product to other reconstructed products are shown in section 3.2.

2.4. Trend Analysis

[30] We used the nonparametric Mann-Kendall [*Mann*, 1945] test for trend significance (p = 0.02, two-tailed), and the *Hirsch et al.* [1982] method to estimate trend slope. Because the controls on streamflow variability operate at varying timescales and in different periods, we applied the trend test to a large number of periods with varying lengths

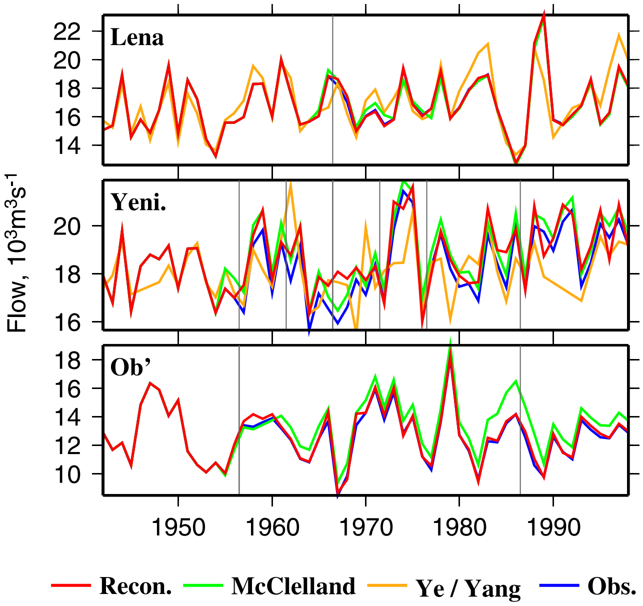

Figure 7. Comparison of annual flows for four reconstructed streamflow products (ours; *McClelland et al.* [2004]; for the Lena, *Ye et al.* [2003]; and for the Yenisei, *Yang et al.* [2004a]) to observed streamflow at the outlets of the Lena, Yenisei, and Ob' river basins. Vertical gray lines indicate the year when filling began for each reservoir in the basin.

and start years between 1937 and 1998. This is defensible because our objective is to determine the causes of observed streamflow changes for different historical periods, rather than to detect change. We examined periods that have a minimum length of 30 years, increasing in length by increments of 5 years. This was done for every start year beginning with 1937. Therefore trends were tested for the following periods: 1937–1967, 1937–1972, 1937–1977, ..., 1938–1968, 1938–1973, 1938–1978, etc... This results in a total of 112 analyzed periods. Trends were calculated using annual, seasonal, and monthly streamflow rates for both observed and reconstructed products. The trend analysis results are reported in section 3.3.

2.5. Reservoir Model Error Propagation

[31] We used satellite-derived reservoir stage estimates for two reservoirs (Lakes Baikal and Bratskoe) to obtain independent estimates of the uncertainty in seasonally averaged reservoir outflow. By making the assumption that the mean uncertainty in stage height for these two reservoirs is representative of the uncertainty for other reservoirs, we estimated the total error in the seasonal reconstructed flows at the basin outlets due to the reservoir simulations (via equations (9)–(11) below). Finally, we compared these errors to the magnitudes of observed changes and trends occurring in the seasonal flows at the basin outlets.

[32] Stage estimates for Lake Baikal (Irkutskoe reservoir) and the Bratskoe reservoir were obtained from the Surface Water Monitoring by Satellite Altimetry database (SWMSA; available at http://www.legos.obs-mip.fr/soa/hydrologie/hydroweb/) for the period 1992 to 1999 (the years of overlap with our reservoir operations). The simulated and SWMSA stage heights were set to the same reference height by subtracting their respective mean annual values from each monthly data point. From these, the root mean square errors (RMSE) were calculated on a monthly basis and then averaged for each season. These values as well as the mean values for the two reservoirs are given in Table 6.

[33] The water balance in a reservoir (assuming no groundwater exchange) between times t_1 and t_2 is given by

$$Qout = Qin + A \cdot (P - E) - \frac{V_2 - V_1}{t_2 - t_1} \qquad (7)$$

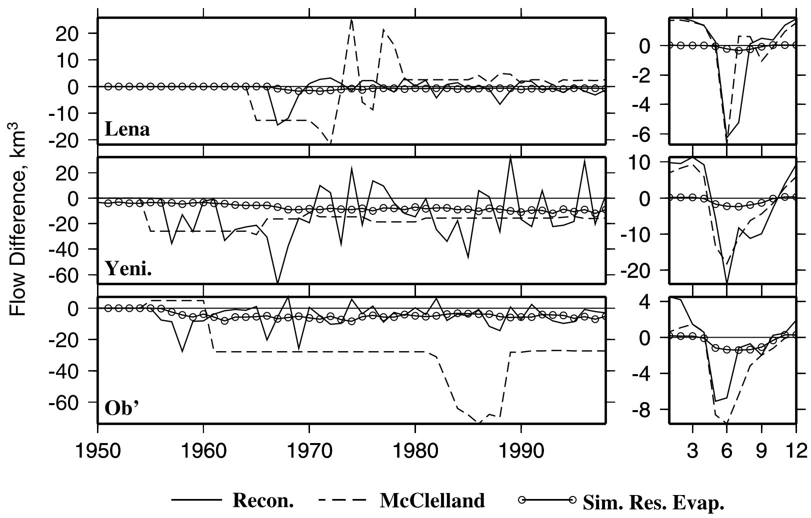

Figure 8. Annual and mean monthly potential reservoir evaporation in the Lena, Yenisei, and Ob' river basins. The negative of the evaporation value is plotted to demonstrate the effects of reservoir evaporation on annual flow. Also plotted are the annual and mean monthly differences between our reconstructed streamflow and observed streamflow and the *McClelland et al.* [2004] streamflow and observed streamflow. Units are $km^3\ a^{-1}$ for annual values and $km^3\ month^{-1}$ for mean monthly values.

Table 8. Annual Reservoir Evaporation Estimates From Three Sources: Berezovskaya et al. (manuscript in preparation, 2007), Our Reconstructed Product, and as Inferred From *McClelland et al.* [2004][a]

	Reservoir Evaporation, $km^3\ a^{-1}$			Percent of Mean Annual Flow		
Basin	Berezovskaya	Reconstructed	McClelland	Berezovskaya	Reconstructed	McClelland
Lena	0.1–0.7	0.8	−2.0	0.02 to 0.12%	0.15%	−0.36%
Yenisei	0.9–3.3	10.1	15.6	0.14 to 0.52%	1.57%	2.43%
Ob'	2.6–4.3	5.3	27.3	0.62 to 1.02%	1.27%	6.47%

[a]The Berezovskaya data are estimates for the year 2000, while the other estimates are for the period of 1990 to 1998.

in which *Qout* and *Qin* are the reservoir outflow and inflow, respectively, *A* is the reservoir surface area, *P* and *E* are the precipitation and evaporation depths over the reservoir, respectively, and V_1 and V_2 are the volumes of the reservoir at times t_1 and t_2, respectively. We want to express the error in *Qout* as a function of the errors in the other variables. For a generic function $q = g(x, \ldots, z)$, the error in *q* is related to the errors in $x, \ldots, z$ as

$$\Delta q = \sqrt{\left(\frac{\partial q}{\partial x}\Delta x\right)^2 + \ldots + \left(\frac{\partial q}{\partial z}\Delta z\right)^2} \quad (8a)$$

and

$$\Delta q \le \frac{\partial q}{\partial x}\Delta x + \ldots + \frac{\partial q}{\partial z}\Delta z \quad (8b)$$

in which equation (8a) holds true if $\Delta x, \ldots, \Delta z$ are independent and random, and equation (8b) gives the upper limit of Δq and holds true for all cases [*Taylor*, 1997]. Therefore the error in *Qout* can be expressed as

$$\Delta Qout = \sqrt{(\Delta Qin)^2 + A^2 \cdot \left[(\Delta P)^2 + (\Delta ET)^2\right] + \frac{(\Delta V_2)^2 + (\Delta V_1)^2}{(t_2 - t_1)^2}} \quad (9a)$$

for independent and random errors, and

$$\Delta Qout \le \Delta Qin + A \cdot (\Delta P + \Delta ET) + \frac{\Delta V_2 + \Delta V_1}{t_2 - t_1} \quad (9b)$$

for all cases. The error in *V* can be determined using equation (4) as

$$\Delta V = \frac{\partial V}{\partial d} \cdot \Delta d = \frac{1}{2} f^2 \cdot d^2 \cdot \Delta d \quad (10)$$

where *d* is the mean depth of the reservoir at the dam between the times of t_1 and t_2, and Δd is the RMSE between simulated and SWMSA stage height (see Table 6). Because the method we used to develop reconstructed streamflow is dependent on the differences between regulated and naturalized simulated streamflow (see section 2.3), the error associated with runoff contributions that enter the stream network downstream of the farthest downstream reservoir on each tributary does not need to be accounted for. Therefore the error in the reconstructed flow at the basin outlet, due only to the reservoir simulations, is a function of the error in *Qout* for each of the *n* farthest downstream reservoirs on each of the contributing tributaries and is given by

$$\Delta Q_{outlet} = \sqrt{\sum_{i=1}^{n} (\Delta Qout_i)^2} \quad (11a)$$

Table 9. Number of Periods (of the 112 Periods Analyzed, See Section 2.4 for Details) for Which Trends Are Significant at 99% for Both Positive and Negative Trends[a]

		Observed		Reconstructed		McClelland	
Time Aggregation	Basin	Increase	Decrease	Increase	Decrease	Increase	Decrease
Annual	Lena	4	0	2	0	2	0
Annual	Yenisei	14	0	4	0	12	0
Annual	Ob'	0	0	0	0	5	0
DJF	Lena	65	0	3	2	0	1
DJF	Yenisei	111	0	14	47	6	3
DJF	Ob'	19	0	0	1	4	0
MAM	Lena	52	0	1	0	2	0
MAM	Yenisei	41	2	19	11	33	6
MAM	Ob'	0	0	0	0	2	0
JJA	Lena	0	0	0	0	1	0
JJA	Yenisei	0	0	16	0	3	0
JJA	Ob'	0	0	0	0	4	0
SON	Lena	0	0	0	0	0	0
SON	Yenisei	0	2	0	0	0	0
SON	Ob'	0	0	0	0	0	0

[a]Trend analysis results are shown for annual and seasonal flows, and for each of the following products: observed (R-ArcticNET [*Lammers and Shiklomanov*, 2000]), our reconstructed product, and the *McClelland et al.* [2004] reconstructed product.

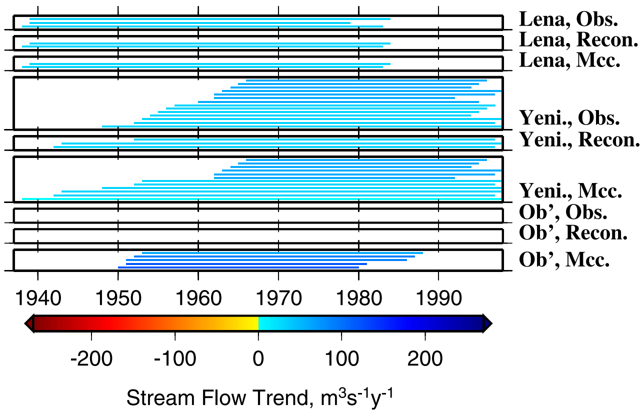

Figure 9. Trends in annual basin-outlet streamflow for significance level 99%. Each line represents a period for which the trend slope is given by the color of the line and the period length is given by the length of the line (starting and ending at the start and end of the period, respectively). Each panel is labeled according to basin and whether the streamflow product is observed ("Obs."), our reconstructed streamflow product ("Recon."), or the *McClelland et al.* [2004] reconstructed streamflow product ("Mcc.").

for independent and random errors, and

$$\Delta Q_{outlet} \leq \sum_{i=1}^{n} \Delta Qout_i \qquad (11b)$$

for all cases. This analysis gives us only a very rough approximation of the uncertainty in the reconstructed flows for several reasons: (1) ΔV, as estimated according to equation (10), is a function not only of Δd but also of the error in equation (4); that is, even if we were able to simulate V with zero error, our estimate of ΔV may be nonzero because of the structural error in equation (4); (2) the satellite-derived stage heights are themselves subject to error; and (3) the stage height errors for Lake Baikal and Bratskoe reservoir are only an approximation for the stage height errors of other reservoirs. The net result may be either an overestimation or underestimation of errors. The results of this analysis are shown and discussed in context of observed changes and trends in section 3.4.

3. Results and Discussion

3.1. Comparison of Simulated and Observed Reservoir Signatures

[34] The green "pluses" associated with the numerals one through ten in Figure 1 are the locations of the gauging stations used to compare our simulated reservoir signature to that inferred from observed streamflow. To calculate the reservoir signature, we compared the mean monthly hydrographs for the period before all upstream reservoirs came online to the mean monthly hydrographs for the period after all upstream reservoirs came online and were filled. Detailed information for each of these gauging stations is given in Table 5. For evaluation at station 9 (Ob' at Novosibirsk), we used separate observed streamflow records for prereservoir and postreservoir construction monthly hydrographs. Because station 9a is downstream of station 9b, and therefore has a larger drainage area, we used the period of overlap (1958 to 1962) as a training period to apply a monthly correction to station 9a streamflow.

[35] The simulated and observed monthly streamflow hydrographs before and after reservoir construction are shown in Figure 4 (column 1). The primary effects are an increase in winter low flow and a decrease in summer peak flow, thereby diminishing streamflow seasonality. The prereservoir and postreservoir construction differences in monthly streamflow (column 2) demonstrate that the reservoir model captures the major features of the effects of reservoir operations on streamflow seasonality. The largest discrepancies between simulated and observed reservoir influences occur during the summer. If the differences are normalized by mean monthly streamflow (column 3), these discrepancies are distributed more uniformly throughout the

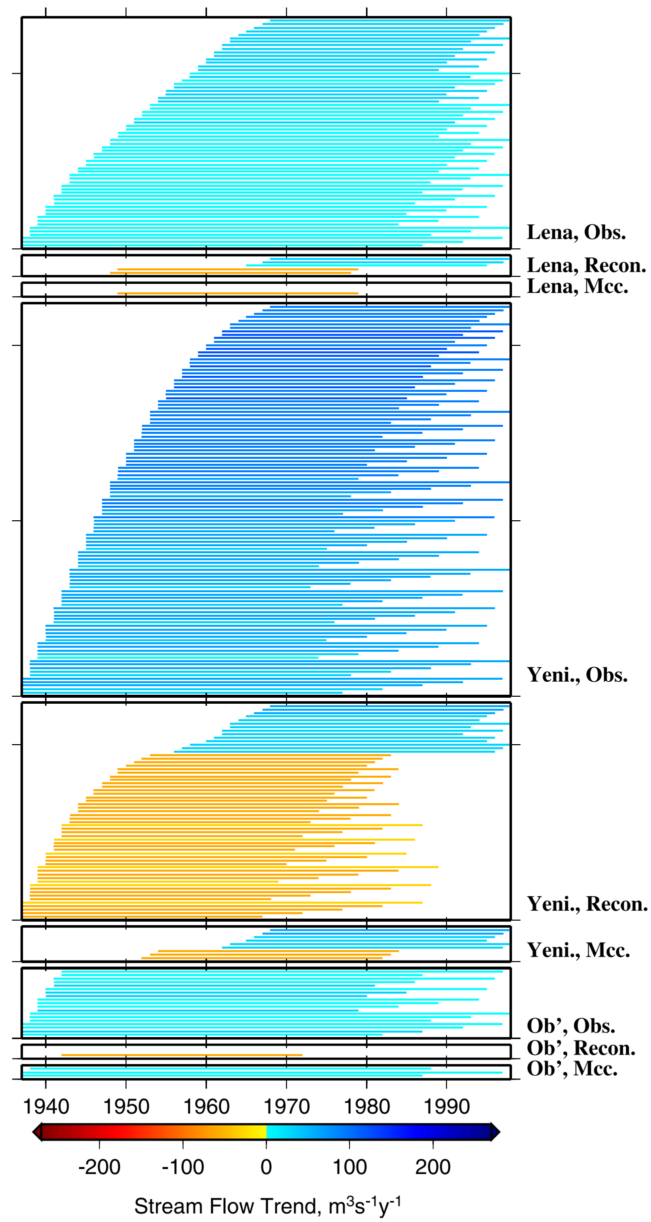

Figure 10. Trends in winter (DJF) basin-outlet streamflow (see Figure 9 caption for explanation).

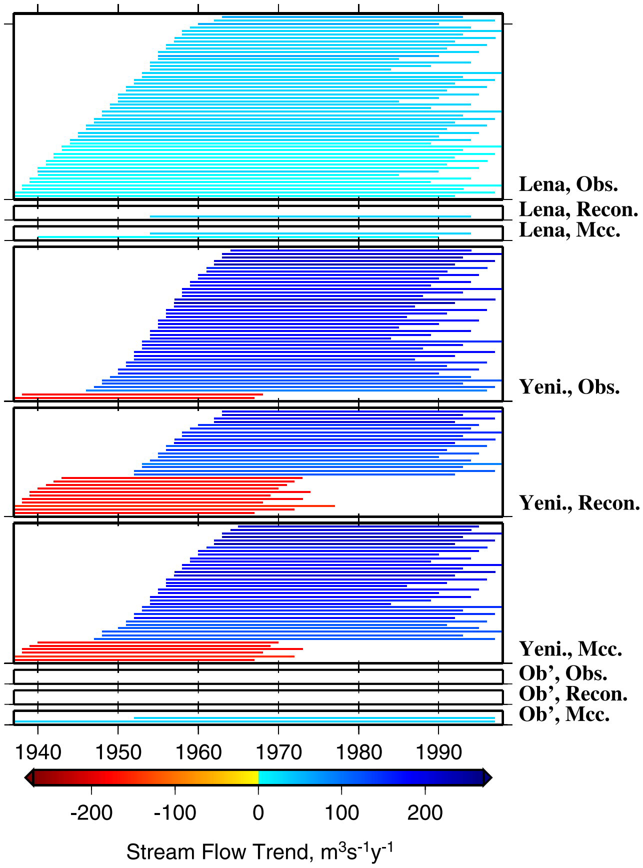

Figure 11. Trends in spring (MAM) basin-outlet streamflow (see Figure 9 caption for explanation).

year. Note that the Ob' simulations do not capture observed seasonality shifts as well as the Lena and Yenisei simulations. This is probably because we do not take into account irrigation demands. Indeed, the only significant irrigation that occurs over the three basins is in the Ob' River basin, of which the basin area is 37% cropland, 2% of which is irrigated [*Revenga et al.*, 1998].

[36] We also examined the effects of reservoir operations on annual streamflow. Table 7 shows the prereservoir and postreservoir construction streamflow rates for both observed and simulated data (for the same periods as above, see Table 5). The table also shows the differences and percent differences (with respect to mean annual flow) in streamflow between the two periods. The simulated and observed changes are generally in the same direction, but the model consistently (with the exceptions of stations 1, 4, and 9) simulates a change that is less (or more negative) than what was observed. It would seem that the model oversimulates the effects of reservoir evaporation on annual flow, especially for the reservoirs on the Angara and Irtish rivers (which are tributaries of the Yenisei and Ob' rivers, respectively). This is expected because reservoir evaporation, although calculated using VIC model simulations of available energy, is subtracted from the energy balance offline, replacing the land surface evaporation that would have occurred had the land not been flooded. Therefore the additional energy required to evaporate at the potential rate is not subtracted from the energy balance. The simulated effects of reservoir evaporation on annual flow should be thought of as an upper bound on the actual effects of reservoir evaporation. Finally, it is important to note that changes that occur between the two periods are not due to reservoir influences only. For example, it is unlikely that the observed increases in annual flow at the outlets of the Lena and Yenisei basins are due to direct human influences. Adam and Lettenmeier (manuscript in preparation, 2007) demonstrate that, without considering excess ground ice, the VIC model does not capture this volume increase and document possible reasons, such as an undersimulation of ground ice melt, which may have contributed to observed streamflow changes. Therefore it is possible that the reservoir model adequately captures the effects of reservoirs on annual flow but that the effects of ground ice melt augmenting annual flow are not captured. The most likely case is

Table 10. Analysis Details for the Longest Period With a Trend Significant at 99% for Annual, Seasonal, and Monthly Observed Streamflows at the Outlet of the Lena Basin (Gauging Station 3 in Figure 1 and Table 5)[a]

				Reconstructed			McClelland		
Time Aggregation	Start Year	End Year	Observed Trend, $m^3\ s^{-1}\ a^{-1}$	Trend, $m^3\ s^{-1}\ a^{-1}$	Significance Passed	Fraction Difference	Trend, $m^3\ s^{-1}\ a^{-1}$	Significance Passed	Fraction Difference
Annual	1939	1989	45.9	46.2	0.98	−0.01	46.2	0.98	−0.01
DJF	1938	1998	21.3	4.8	0.80	**0.77**	4.9	0.80	**0.77**
MAM	1938	1998	25.8	17.3	0.95	0.33	17.3	0.98	0.33
Jan	1938	1998	19.8	3.9	–	**0.80**	3.7	0.60	**0.81**
Feb	1938	1998	24.9	8.8	0.95	**0.65**	7.9	0.98	**0.68**
Mar	1938	1998	25.1	11.3	0.99	**0.55**	9.0	0.99	**0.64**
Apr	1938	1998	21.0	9.4	0.99	**0.55**	6.8	0.99	**0.68**
May	1954	1994	98.5	95.4	0.99	0.03	111.3	0.99	−0.13
Nov	1938	1998	20.3	6.6	0.60	**0.67**	10.0	0.90	**0.51**
Dec	1938	1998	17.9	2.0	–	**0.89**	2.5	–	**0.86**

[a]Seasons or months for which none of the analyzed 112 periods had a significant trend are not included in the table. Column 4 is the trend magnitude for observed streamflow (R-ArcticNET [*Lammers and Shiklomanov*, 2000]). Columns 5 through 7 are trend magnitude, most strict significance level passed, and the difference between the reconstructed and observed trends expressed as a fraction of the observed trend for our reconstructed product. Columns 8 through 10 are trend magnitude, most strict significant level passed, and the difference between the reconstructed and observed trends expressece as a fraction of the observed trend for the *McClelland et al.* [2004] reconstructed product. Significance levels tested are 0.99, 0.98, 0.95, 0.90, 0.80, and 0.60. Trends not passing 0.60 significance are indicated by dashes. Fractional differences are shown in bold if they exceed 0.5.

Table 11. Analysis Details for the Longest Period With a Trend Significant at 99% for Annual, Seasonal, and Monthly Observed Streamflows at the Outlet of the Yenisei Basin (Gauging Station 7 in Figure 1 and Table 5)[a]

				Reconstructed			McClelland		
Time Aggregation	Start Year	End Year	Observed Trend, $m^3\ s^{-1}\ a^{-1}$	Trend, $m^3\ s^{-1}\ a^{-1}$	Significance Passed	Fraction Difference	Trend, $m^3\ s^{-1}\ a^{-1}$	Significance Passed	Fraction Difference
Annual	1948	1998	30.0	34.5	0.98	−0.15	36.4	0.99	−0.21
DJF	1938	1998	79.6	−2.5	–	**1.03**	9.9	0.90	**0.88**
MAM	1948	1998	135.5	77.9	0.95	0.42	122.4	0.99	0.10
SON	1937	1982	−36.1	−5.9	–	**0.84**	−20.4	0.80	0.44
Jan	1938	1998	79.4	−4.7	–	**1.06**	9.4	0.90	**0.88**
Feb	1938	1998	96.4	12.6	0.90	**0.87**	16.3	0.99	**0.83**
Mar	1938	1998	106.2	11.0	0.60	**0.90**	21.0	0.99	**0.80**
Apr	1938	1998	122.0	42.8	0.99	**0.65**	68.9	0.99	0.44
May	1938	1978	−431.0	−430.0	0.98	0.00	−380.9	0.95	0.12
Jul	1946	1986	−190.9	−77.3	0.60	**0.59**	−39.6	–	**0.79**
Aug	1938	1998	−57.6	32.7	0.80	**1.57**	−9.9	–	**0.83**
Sep	1944	1994	−75.0	12.9	–	**1.17**	−38.7	0.80	0.48
Oct	1937	1992	−50.0	−3.9	–	**0.92**	−37.0	0.90	0.26
Nov	1938	1998	55.1	20.1	0.90	**0.63**	26.4	0.99	**0.52**
Dec	1938	1998	64.6	−13.5	0.90	**1.21**	10.4	0.80	**0.84**

[a]See Table 10 caption for further information.

that both explanations pertain in varying degrees for each basin.

3.2. Comparison to Other Reconstructed Streamflow Products

3.2.1. Descriptions of Other Products

[37] In section 2.3 we describe the development of our reconstructed streamflow product, for which the simulated effects of reservoirs were removed from the observed streamflow. Other reconstructed products exist for these basins which were derived purely from observed streamflow data. The *McClelland et al.* [2004] product is for the outlets of all three basins (as well as the Kolyma basin which is also regulated), while the *Ye et al.* [2003] and *Yang et al.* [2004a] products are for the Lena and Yenisei basins, respectively.

[38] The *McClelland et al.* [2004] product was created by comparing the gauged discharge data before and after dam construction (for stations at or near the reservoirs) and applying the monthly differences to the downstream discharge. For the periods during reservoir filling, data were reconstructed on a year-by-year basis relative to the predam average to allow for large interannual changes in discharge due to the filling process. Differences were subtracted from downstream values in months showing excess discharge after reservoir filling and were added to the downstream values in months showing deficits in discharge after reservoir filling. The authors note two possible limitations to this method. First, they assumed that all changes in average streamflow (upstream of the stations) are attributed only to reservoirs, although they argue that the long-term effects of climate on streamflow are negligible compared to the effects of the reservoirs. Furthermore, the fraction of watershed area upstream of the stations used for analysis is small compared to the downstream fraction (especially for the Lena and Ob’), and climate change effects on streamflow generated in the downstream fraction are represented [*McClelland et al.*, 2004]. Second, there were no corrections for time lags, i.e., the travel time of streamflow between the dam and the gauging station near basin outlet, which can be up to 2 months. From here on, we will refer to this product as “McClelland.”

[39] *Ye et al.* [2003] and *Yang et al.* [2004a] use a paired basin method to create reconstructed streamflow for the Lena and Yenisei basins, respectively. This method consists of three steps.

[40] 1. Stepwise regression was used to select input streamflow variables. For lags of 0 to 2 months (to reflect

Table 12. Analysis Details for the Longest Period With a Trend Significant at 99% for Annual, Seasonal, and Monthly Observed Streamflows at the Outlet of the Ob’ Basin (Gauging Station 10 in Figure 1 and Table 5)[a]

				Reconstructed			McClelland		
Time Aggregation	Start Year	End Year	Observed Trend, $m^3\ s^{-1}\ a^{-1}$	Trend, $m^3\ s^{-1}\ a^{-1}$	Significance Passed	Fraction Difference	Trend, $m^3\ s^{-1}\ a^{-1}$	Significance Passed	Fraction Difference
DJF	1938	1998	20.8	−5.6	0.60	**1.27**	16.3	0.98	0.22
Jan	1938	1998	20.0	−13.6	0.80	**1.68**	15.8	0.98	0.21
Feb	1938	1998	22.0	−9.1	0.60	**1.42**	14.0	0.99	0.36
Mar	1938	1998	22.8	7.3	0.90	**0.68**	11.9	0.99	0.48
Apr	1938	1998	21.1	15.8	0.99	0.25	13.8	0.99	0.34
Jun	1951	1981	185.7	219.3	0.90	−0.18	360.0	0.99	−0.94
Nov	1963	1998	89.1	82.3	0.98	0.08	85.2	0.98	0.04

[a]See Table 10 caption for further information.

Table 13a. Analysis of the Error in Reconstructed Yenisei River Streamflow Due to Uncertainties in the Reservoir Simulations: Angara Tributary[a]

	Reservoir											
	Irkutskoe				Bratskoe				Ust'-Ilimskoe			
Season	ΔQin	ΔP, ΔE	ΔdV/dt	ΔQout	ΔQin	ΔP, ΔE	ΔdV/dt	ΔQout	ΔQin	ΔP, ΔE	ΔdV/dt	ΔQout
DJF	0.30	0.11	0.44	0.54	0.54	0.02	1.61	1.70	1.70	0.01	0.32	1.73
MAM	0.44	0.15	1.48	1.55	1.55	0.02	1.40	2.09	2.09	0.01	0.31	2.11
JJA	0.14	0.17	1.36	1.37	1.37	0.03	1.62	2.12	2.12	0.01	0.34	2.15
SON	0.34	0.15	1.25	1.30	1.30	0.02	1.51	1.99	1.99	0.01	0.32	2.02

[a]All units are in 10^3 m^3 s^{-1}. See text for details. Note that "ΔP, ΔE" = A · $(\Delta P^2 + \Delta E^2)^{1/2}$ where A is obtained from Table 1, and "ΔdV/dt" = $(\Delta V_2^2 + \Delta V_1^2)^{1/2}$ / $(t_2 - t_1)$, where "2" refers to the current season and "1" refers to the previous season.

the time of flow routing within the basin), the authors calculated correlations between streamflow from basins that are unregulated and streamflow at the basin outlet for the prereservoir period. The lag times that produced the highest correlations were selected.

[41] 2. A multiple least squares regression approach was applied to obtain the best relationship for each month. Results were reasonable for all months except May for the Lena basin, for which an exponential model was applied.

[42] 3. Monthly streamflow data from the unregulated basins were used in the regression relationships to obtain a reconstructed monthly discharge time series at the outlet of the regulated basin for the full study period (1942 to 1999 for the Lena, and 1936 to 1999 for the Yenisei). Reconstructed streamflow was not produced for the Ob' River basin because of complications due to irrigation and other water uses and diversions (D. Yang, personal communication, 2006). From here on, we will refer to these products as "Ye/Yang."

3.2.2. Comparison of Reservoir Effects on Flow Seasonality

[43] Figure 5 shows the monthly reservoir signatures inferred from each of the three reconstructed streamflow products. These signatures were calculated by subtracting the observed mean monthly hydrograph from the reconstructed mean monthly hydrograph for the postreservoir period (column 1). Whereas the signatures from our product and that of McClelland have very similar shapes for the Lena and Yenisei basins, the Ye/Yang signature is much different from the others in the summer. The winter low flow comparison is more easily seen by examining the percent changes in monthly streamflow, which we calculated by normalizing the absolute differences by mean monthly observed streamflow (column 2). Although the three products were constructed using completely different methodologies, they imply very similar effects on winter low flows for the Lena and Yenisei basins. This is an indication that the primary human influence in these basins is through reservoir construction for hydropower production. For the Ob' basin, the signatures from our product and that of McClelland, although sharing general features such as an increase in winter streamflow and a decrease in summer streamflow, have some significant discrepancies. For example, our product suggests a much larger effect on winter flows. As mentioned earlier, these discrepancies are likely due to more complicated water uses in this basin, which affect our ability to accurately simulate human effects on streamflow while only considering hydropower production.

[44] Seasonal streamflow time series for each of the reconstructed products and the observed data are shown in Figure 6. The year that reservoirs for each basin came online and began to fill are shown by gray vertical lines in each of the figures. By construct, our product and the McClelland product are identical to observed streamflow before reservoir filling. Because the Ye/Yang products for the complete period (prereservoir and postreservoir) were created by paired basin analysis, these products do not necessarily match observed streamflow before reservoir implementation. All products show that the most significant changes occur during the winter season. Although these products show similar long-term winter changes for the Lena and Yenisei basins, the timing during the filling period is slightly different. In both cases, our product shows a more abrupt decrease in winter streamflow after the construction of each additional reservoir, which may indicate that we constrain the reservoir minimum outflow to be too large during the filling period, thus precluding winter flow to contribute to reservoir filling. The behavior of the three

Table 13b. Same as Table 13a but for Yenisei (Above Angara Confluence)[a]

	Reservoir							
	Sayano-Shushenskoe				Krasnoyarskoe			
Season	ΔQin	ΔP, ΔE	ΔdV/dt	ΔQout	ΔQin	ΔP, ΔE	ΔdV/dt	ΔQout
DJF	0.06	0.00	0.10	0.12	0.12	0.01	0.09	0.15
MAM	0.19	0.00	0.09	0.21	0.21	0.01	0.04	0.21
JJA	0.11	0.00	0.10	0.15	0.15	0.01	0.09	0.18
SON	0.14	0.00	0.11	0.18	0.18	0.01	0.12	0.22

[a]All units are in 10^3 m^3 s^{-1}. See text for details. Note that "ΔP, ΔE" = A · $(\Delta P^2 + \Delta E^2)^{1/2}$ where A is obtained from Table 1, and "ΔdV/dt" = $(\Delta V_2^2 + \Delta V_1^2)^{1/2}$ / $(t_2 - t_1)$, where "2" refers to the current season and "1" refers to the previous season.

Table 13c. Same as Table 13a but for Kureika Tributary[a]

Season	Kureiskoe Reservoir			
	ΔQin	ΔP, ΔE	ΔdV/dt	ΔQout
DJF	0.05	0.00	0.08	0.09
MAM	0.04	0.00	0.05	0.07
JJA	0.14	0.00	0.04	0.14
SON	0.10	0.00	0.07	0.12

[a]All units are in 10^3 m^3 s^{-1}. See text for details. Note that "ΔP, ΔE" = A · $(\Delta P^2 + \Delta E^2)^{1/2}$ where A is obtained from Table 1, and "ΔdV/dt" = $(\Delta V_2^2 + \Delta V_1^2)^{1/2} / (t_2 - t_1)$, where "2" refers to the current season and "1" refers to the previous season.

reconstructed products during the spring, summer, and fall for the Lena and Yenisei basins are fairly similar, with the exception that the Ye/Yang products tend to have a greater interannual variability for all seasons except for winter, as was noted earlier. This may be an artifact of the paired basin analyses; that is, fall Ye/Yang flows for the Lena in particular show ''peakier'' variations than observed for the prereservoir period. As discussed earlier, larger discrepancies between the two reconstructed products exist for the Ob' basin, particularly for winter and summer, the seasons most influenced by reservoirs.

3.2.3. Comparison of Reservoir Effects on Annual Flows

[45] Annual time series for each of the reconstructed products and the observed data are shown in Figure 7. As discussed earlier, Ye/Yang used paired basin analysis to produce a reconstructed product. This makes it difficult to ascertain what divergences between the reconstructed and observed data after reservoir construction are due to reservoir effects as opposed to variability inherent in the paired basin analyses. Therefore we focus the following discussion on the comparison of our reconstructed product to that of McClelland. Figure 7 suggests that the primary effects of the Vilyuiskoe reservoir on Lena annual flow occurred immediately after filling. Our product diverges significantly from observations for 5 years after reservoir construction, whereas the McClelland product diverges from observed for about 10 years. In the Yenisei, the interannual effects of reservoirs are more complex because of numerous reservoirs coming online over a 30-year period. For the Ob' and the Yenisei basins, our product and that of McClelland both show significant reservoir evaporation influences in that the reconstructed products maintain a higher annual streamflow after filling completion.

[46] To better interpret the effects of reservoir evaporation, we plot the differences between observed and reconstructed flow for our product and the McClelland product (Figure 8). Also included in this plot are our simulated reservoir evaporation estimates summed over each basin. For McClelland, inferred reservoir evaporation can be estimated as the long-term difference between reconstructed and observed annual streamflow by assuming that all changes to the annual flow regime for areas upstream of the reservoirs (after filling) are due only to reservoir evaporation. This is not a robust assumption as can be seen in Figure 8; the McClelland product infers a negative evaporation over the Lena basin, indicating that other factors are indeed likely occurring in the basin headwaters to change the annual flow regime. These annual losses of reservoir storage to evaporation are given in Table 8 along with the year 2000 estimates of Berezovskaya et al. (manuscript in preparation, 2007). Berezovskaya et al. based their estimates on those of *Shiklomanov and Veretennikova* [1978] (which were derived from mean evaporation maps), but reduced the values to account for the overestimation of predicted reservoir storage by the end of the last century. Our estimates are greater than those of Berezovskaya et al. As mentioned in section 3.1, we are likely oversimulating reservoir evaporation, which would suggest that the Berezovskaya et al. estimates may provide a realistic range of values. The McClelland flows for the Ob' basin show considerably higher evaporation effects than our reconstructed product, which may be an indication that evaporation rates have increased over the land surface in the Ob' headwaters; that is, not all of the increased evaporation inferred by the McClelland product is due to reservoir construction. To a lesser degree, this may be true for the Yenisei basin as well.

3.3. Effect of Reservoirs on Streamflow Trends

[47] As described in section 2.4, annual and seasonal flows for observed and two reconstructed products (ours and that of McClelland) were tested for trend for periods with varying lengths and start years between 1937 and 1998. The resulting signs of the trends for annual and seasonal flows are summarized in Table 9. Generally, annual flows are increasing, primarily for the Lena and Yenisei basins. Winter and spring are the seasons with significant observed streamflow increases, although in many cases these trends are likely due to reservoir effects; that is, trends for the reconstructed products are both positive and negative. We explored these results in depth by plotting the magnitude for each of the trends (that passed

Table 13d. Same as Table 13a but for Yenisei at Igarka (Outlet)[a]

Season	Errors		Flow Differences			Seasonal Trends (Significant at 99%)		
	$\Delta Q_{outlet}{}^{I}$	$\Delta Q_{outlet}{}^{M}$	Flow Difference	$\lvert Diff \rvert/\Delta Q_{outlet}{}^{Ib}$	$\lvert Diff \rvert/\Delta Q_{outlet}{}^{Mb}$	Total Number[b]	Number $\geq \Delta Q_{outlet}{}^{Ib}$	Number $\geq \Delta Q_{outlet}{}^{Mb}$
DJF	1.74	4.34	2.98	1.71	0.69	111	93%	20%
MAM	2.13	5.70	3.19	1.50	0.56	43	100%	95%
JJA	2.16	5.69	−3.80	1.76	0.67	0	–	–
SON	2.03	5.62	−2.65	1.30	0.47	2	0%	0%

[a]Unless marked with a footnote, all units are in 10^3 m^3 s^{-1}. See text for details.
[b]These values are unitless.

Table 14a. Analysis of the Error in Reconstructed Ob' River Streamflow Due to Uncertainties in the Reservoir Simulations: Ob' (Above Irtish Confluence)[a]

	Novosibirskoe Reservoir			
Season	ΔQin	ΔP, ΔE	ΔdV/dt	ΔQout
DJF	0.07	0.00	0.12	0.14
MAM	0.37	0.00	0.03	0.37
JJA	0.14	0.01	0.13	0.19
SON	0.10	0.00	0.17	0.20

[a]See text and Tables 13a–13d captions for details.

99% significance) for each basin. The annual trends are shown in Figure 9. Positive flow trends at the Lena outlet between the mid 1930s and the mid 1980s are persistent for both the observed and reconstructed products, indicating that this increase is not associated with reservoirs. Furthermore, long-term flow trends at the Yenisei outlet between the 1940s/1950s and the end of last century are also persistent for all products, but larger trends in the later years for the observed product could be a result of reservoir filling effects on interannual variability (e.g., the flow will increase once reservoir filling is complete for each of the reservoirs). This cannot be stated conclusively, however, because our reconstructed product does not exhibit these shorter larger trends, suggesting that they may be a result of reservoir filling. On the other hand, the McClelland product does, suggesting that the trends are natural. We did not detect any long-term annual trends over the Ob' for either the observed data or for our product. The McClelland product exhibits positive trends in the middle of the period, which are consistent with the product having larger annual flows than the other products after the 1950s and 1980s, and we suspect may be a result of inclusion of upstream effects in the McClelland algorithm that are not entirely reservoir-induced (see section 3.2.3).

[48] We show trend plots for the two more interesting seasons: winter and spring (Figures 10 and 11, respectively). Both reconstructed products indicate that the persistent positive trends for periods starting earlier than the 1960s in Lena and Yenisei winter flow are primarily due to reservoirs. Positive winter trends beginning in the 1960s for the Lena and the Yenisei basins may be only partially due to reservoirs; for example, a decrease in the ratio of solid to liquid precipitation and an increase in permafrost active layer depth are both hypotheses to explain the remainder of the winter changes. The reconstructed data suggest that Lena and Yenisei winter flows were naturally decreasing in the early part of the record, but increasing between the 1950s/1960s and the end of the last century. Results for Ob' winter flow trends are less conclusive. Whereas our product suggests that long-term trends were entirely due to reservoir operations, the McClelland data suggest that long-term trends starting in the 1930s may be natural. These results are similar to those for spring flow trends (Figure 11). Both products suggest that the persistent positive trends in the Lena spring flow are due to reservoirs. Alternatively, the two reconstructed products both exhibit very similar patterns of change to that of the observed product for the Yenisei basin, with negative trends in the early period of the record and persistent positive trends starting around 1950, suggesting that these changes are not reservoir-induced. Once again, the Ob' results are less conclusive with only the McClelland product exhibiting long-term positive trends. We do not show results for summer and fall because there are fewer significant changes during these seasons. The only noteworthy features are persistent positive trends in Yenisei summer flow between the 1940s and the 1970s for both reconstructed products, whereas there are no significant trends for the observed product, suggesting that reservoir effects countered these changes. Also negative trends in Yenisei fall flow between the 1940s and the 1980s are apparent in the observed product but not in the reconstructed products, indicating that these trends are reservoir-induced.

[49] We estimated the fractions of the statistically significant trend magnitudes in the observed data that may be due to reservoir effects. The longest period for which the observed trend was significant (99%) was selected for each time aggregation interval (i.e., annual, seasonal, and monthly) for each basin. The reconstructed products were then tested for trend for this same period. If there were no significant long-term (≥30 years) observed trends, results for this time interval are not shown (e.g., for the Ob', annual, spring, summer, fall, etc...). The streamflow trend magnitudes from the observed data and two of the reconstructed products are given in Tables 10, 11, and 12 for the Lena, Yenisei, and Ob' basins, respectively. The difference between the observed trend magnitude and the reconstructed trend magnitudes provides estimates of the fraction of the observed trend that was reservoir-induced.

[50] The two reconstructed products produce similar results for the Lena basin, accounting for 77% of the observed winter trend and 33% of the observed spring trend (primarily for March and April), but little of the observed annual trend. The two products are in less but still similar agreement for the Yenisei basin. Both products indicate that reservoirs are mostly (>88%) responsible for the observed winter trend. Furthermore, they may account for between 44% and 90% of early spring (March and April) trends, and potentially 26% to over 100% of late summer and fall trends. Like the Lena, the reservoirs appear to account for none of the Yenisei observed annual trend; in fact the reservoirs reduced the annual trend by 15% to 21%, likely because of increased evaporation. The two reconstructed products are in much less agreement for the Ob', with our product suggesting that most or all of the change in January through March are due to reservoirs, whereas the

Table 14b. Same as Table 14a but for Irtish Tributary[a]

	Reservoir							
	Bukhtarminskoe				Shul'binskoe			
Season	ΔQin	ΔP, ΔE	ΔdV/dt	ΔQout	ΔQin	ΔP, ΔE	ΔdV/dt	ΔQout
DJF	0.04	0.02	0.50	0.50	0.50	0.00	0.02	0.50
MAM	0.16	0.02	0.47	0.50	0.50	0.00	0.01	0.50
JJA	0.04	0.03	0.56	0.56	0.56	0.00	0.03	0.56
SON	0.04	0.02	0.53	0.53	0.53	0.00	0.04	0.53

[a]See text and Tables 13a–13d captions for details.

Table 14c. Same as Table 14a but for Ob' at Salekhard (Outlet)[a]

	Errors		Flow Differences			Seasonal Trends (Significant at 99%)		
Season	$\Delta Q_{outlet}{}^{I}$	$\Delta Q_{outlet}{}^{M}$	Flow Difference	$\lvert Diff\rvert/\Delta Q_{outlet}{}^{Ib}$	$\lvert Diff\rvert/\Delta Q_{outlet}{}^{Mb}$	Total Number[b]	Number $\geq \Delta Q_{outlet}{}^{Ib}$	Number $\geq \Delta Q_{outlet}{}^{Mb}$
DJF	0.52	1.02	0.85	1.61	0.83	19	100%	100%
MAM	0.62	1.29	2.19	3.51	1.70	0	–	–
JJA	0.59	1.20	−0.06	0.10	0.05	0	–	–
SON	0.57	1.24	−1.83	3.20	1.48	0	–	–

[a]See text and Tables 13a–13d captions for details.
[b]These values are unitless.

McClelland product indicates that between 21% and 48% of these changes are due to reservoirs. They both produce greater June trends than observed, indicating that reservoirs acted to decrease the natural June flow increases.

3.4. Reservoir Model Error Propagation

[51] In section 2.5 we describe the equations used to propagate error in our reservoir simulations to the basin outlet. The results of the error propagation analysis are given in Tables 13a–13d, Tables 14a–14c, and Tables 15a and 15b for the Yenisei, Ob', and Lena river basins, respectively. Tables 13a–13c, 14a, 14b, and 15a each give the results for one of the basin's tributaries that is regulated by one or more large dams (with the exception of the Khantaika tributary because it enters the Yenisei River downstream of the gauging station we used for analysis). There are four columns for each reservoir on that tributary, one for each of the terms in equation (9a). ΔQin for the farthest upstream reservoir on each tributary was approximated using the best available information for streamflow measurement errors in these basins. *Shiklomanov et al.* [2006] estimated the measurement error on a monthly basis at the outlets of the Lena, Yenisei, and Ob' river basins (among others). Averaging over each of the four seasons (DJF, MAM, JJA, and SON) results in the following errors: 17.0%, 15.6%, 4.3%, and 11.2% for the Lena; 17.9%, 15.9%, 3.3%, and 12.0% for the Yenisei; and 16.0%, 15.1%, 4.6%, and 8.9% for the Ob', expressed as the percent of flow. Although these values do not necessarily apply to streamflow measurements other than at the basin outlets, we used them as the best estimates of error for streamflow at the upstream gauging stations in each basin. For the remaining reservoirs, ΔQin was set equal to $\Delta Qout$ of the upstream reservoir. The interreservoir contributions of runoff are generally small in comparison to $Qout$, therefore we neglect the error associated with these contributions. Other than for Lake Baikal (Irkutskoe reservoir) which has a very large surface area, ΔP and ΔE are negligible. Therefore the errors we attribute to P and E contributions to/from the water balance have little effect on the final error estimates. We apply a rough error estimate of 20% of mean seasonal P for both terms (recall that precipitation has already been adjusted for systematic bias).

[52] An addition, Tables 13d, 14c, and 15b provide estimates of the error at the gauging station nearest to the basin outlet. They are divided into three groups: errors in seasonal flows, seasonal differences in flow as a result of reservoirs, and trends in seasonal flows. The first group gives ΔQ_{outlet} as calculated via equation (11a) (ΔQ^{I}_{outlet}) and equation (11b) (ΔQ^{M}_{outlet}), where I indicates the case of independent and random errors while M indicates maximum error. These values were calculated using the $\Delta Qout$ estimates for the farthest downstream reservoir on each tributary (i.e., the last column for Tables 13a–13c, 14a, 14b, and 15a). In the second group are simulated flows for the period of 1931 to 1955 (before all reservoirs were constructed) subtracted from simulated flows for the period of 1988 to 1999 (after all reservoirs were filled) in the first column (i.e., reservoir signature), and these absolute differences divided by the two estimates of ΔQ_{outlet} in the second and third columns. In the third group are the numbers of periods for which observed streamflow trends are significant at 99% (also see Table 9) in the first column, and in the second and third columns are the percentages of these numbers of periods for which the trend magnitudes exceed ΔQ_{outlet} in absolute value, for both estimates of ΔQ_{outlet}. The purpose of Tables 13d, 14c, and 15b is to show, at the outlet of each basin, (1) the relative value of seasonal flow differences due to reservoir regulation compared to the error due to reservior modeling and (2) the relative values of seasonal flow trends compared to the error due to reservoir modeling.

[53] For the Yenisei basin (Tables 13a–13d), ΔQ^{I}_{outlet} is less than the simulated reservoir signature on seasonal streamflow for all seasons, although ΔQ^{M}_{outlet} exceeds the reservoir signature for all seasons. Therefore, in the more likely case that the errors in each of the terms in equations (9) and (11) are independent and random, the signal exceeds the noise. In the worst case scenario in which the errors are dependant or systematically biased, the noise may exceed the signal. Regarding trends, ΔQ^{I}_{outlet} is less than most to all of the significant winter and spring trends, and greater than both of the fall trends, while ΔQ^{M}_{outlet} is less than most of the spring trends and less than only 20% of the winter trends. Therefore comparisons between observed and

Table 15a. Analysis of the Error in Reconstructed Lena River Streamflow Due to Uncertainties in the Reservoir Simulations: Vilyui Tributary[a]

	Vilyuiskoe Reservoir			
Season	ΔQin	ΔP, ΔE	ΔdV/dt	ΔQout
DJF	0.00	0.01	0.14	0.14
MAM	0.12	0.01	0.08	0.15
JJA	0.07	0.01	0.14	0.15
SON	0.04	0.01	0.18	0.18

[a]See text and Tables 13a–13d captions for details.

Table 15b. Same as Table 15a but for Lena at Kusur (Outlet)[a]

	Errors		Flow Differences			Seasonal Trends (Significant at 99%)		
Season	ΔQ_{outlet}^{I}	ΔQ_{outlet}^{M}	Flow Difference	$\lvert Diff\rvert/\Delta Q_{outlet}^{Ib}$	$\lvert Diff\rvert/\Delta Q_{outlet}^{Mb}$	Total Number[b]	Number $\geq \Delta Q_{outlet}^{Ib}$	Number $\geq \Delta Q_{outlet}^{Mb}$
DJF	0.14	0.21	0.78	5.49	3.75	65	100%	100%
MAM	0.15	0.23	1.21	8.27	5.19	52	100%	100%
JJA	0.15	0.24	1.18	7.64	4.87	0	–	–
SON	0.18	0.30	−0.41	2.30	1.37	0	–	–

[a]See text and Tables 13a–13d captions for details.
[b]These values are unitless.

reconstructed streamflow trends for the Yenisei basin may be robust for spring, unreliable for fall, and should be interpreted with caution for winter. Similarly, for the Ob' basin (Tables 14a–14c), ΔQ_{outlet}^{I} is less than the reservoir signature for all seasons but summer, and ΔQ_{outlet}^{M} is less than the reservoir signature for all seasons except winter and summer. Regarding trends, ΔQ_{outlet}^{M}, and thus ΔQ_{outlet}^{I}, are less than all of the significant winter trends. There were no significant trends for the other seasons. As mentioned in section 2.5, these error estimates are particularly unreliable for the Ob' basin because the error estimates in stage height, which were derived from two of the Yenisei reservoirs, may not be applicable to the Ob' reservoirs which are partially operated for irrigation purposes. For the Lena basin (Tables 15a and 15b), both estimates of ΔQ_{outlet} are less than the reservoir signature for all seasons. Similarly, both estimates of ΔQ_{outlet} are less than all significant winter and spring trends, while no significant trends were detected for the other seasons. Of the three basins, comparisons between observed and reconstructed streamflow trends for the Lena basin may be the most robust.

4. Conclusions

[54] We have estimated the influence of reservoirs on long-term annual, seasonal, and monthly trends at the outlets of the Lena, Yenisei and Ob' river basins. Although reservoirs appear to have had little effect on annual trends, we conclude that they are responsible for much of the seasonal changes that have been observed, especially during the winter and early spring. Results for the three basins are as follows:

[55] 1. For the Lena, we conclude that the positive long-term (1938–1998) trend in the observed Lena winter flow at basin outlet is primarily due to the construction and operation of the reservoir at the headwaters of the Vilyui tributary, accounting for approximately 80% of the observed trend. This reservoir accounts for approximately 30% of the observed spring trend (primarily because of reservoir-induced increases in March and April).

[56] 2. For the Yenisei, whereas the positive observed winter trend at the basin outlet persists for the entire observational record, our results suggest that winter flows were naturally decreasing in the early part of the record, and increasing between the 1960s and the end of the last century. Analysis over the long term (1938–1998) shows that the positive observed winter trend for this period is due to reservoir influences. Both observed and reconstructed spring trends are negative in the earliest part of the record, followed by a positive trend beginning around 1950. For the period of 1948 to 1998, reservoir influences may account for approximately 40% of the positive observed spring trend (primarily during March and April, i.e., reservoir influences in May are negligible). Negative observed trends occurring during July to October are also primarily due to reservoir influences by as much as 60% to over 100%, depending on the month. Also, August and September trends would have been positive (yet insignificant) over the long term, were it not for reservoir influences.

[57] 3. For the Ob', most or all (>70%) of the changes in the winter and early spring (i.e., March) are possibly due to reservoirs. Our reconstructed product exhibits a greater June trend than observed, indicating that reservoirs acted to decrease natural June flow increases (by approximately 20% of the reconstructed flow trend).

[58] When evaluating the effects of climate on historical streamflow changes, it is critical that reservoir effects be considered, as the reservoirs can cause changes to the streamflow regime that are similar to long-term climate effects. By isolating the direct human effects on the streamflow regime of these Siberian basins, it becomes possible to examine what natural changes have occurred in order to further our understanding of how climate change has affected runoff generation in the Arctic. For example, trend analysis of the reconstructed streamflows demonstrates that the following changes were likely due to climatic influences: long-term (spanning more than 40 years) increases in Lena and Yenisei annual streamflow; decreases in Lena and Yenisei winter streamflow for periods starting in the 1940s and ending in the 1970s and 1980s, followed by increases for periods starting in the 1950s and 1960s and ending in the 1990s; decreases in Yenisei spring streamflow for periods starting in the 1930s and ending around 1970, followed by increases for periods starting in the 1950s and 1960s and ending in the 1990s; and increases in Yenisei summer streamflow for periods starting in the 1940s and ending in the 1970s. We detected few significant trends in Ob' seasonal or annual reconstructed streamflow, although there are some significant trends for individual months (e.g., a positive trend existed in 1938 to 1998 April streamflow). In a companion paper [*Adam and Lettenmaier*, 2007], we apply these reconstructed data to formulate a hypothesis on how precipitation and temperature changes have jointly contributed to streamflow changes in the Eurasian Arctic; and in the work by Adam and Lettenmaier (manuscript in preparation, 2007), we test this hypothesis by exploring the sensitivity of streamflow to precipitation and temperatures changes using the model described in section 2.2.1. By improving our understanding of the causes of historical streamflow trends, we will be able to more accurately

predict how the streamflow regime in the Eurasian Arctic will be affected by predicted climate change.

[59] **Acknowledgments.** This research was supported by NSF grant OP-0230372 to the University of Washington. We would like to thank three anonymous reviewers whose thoughtful comments improved this manuscript.

References

Adam, J. C., and D. P. Lettenmaier (2003), Adjustment of global gridded precipitation for systematic bias, *J. Geophys. Res.*, *108*(D9), 4257, doi:10.1029/2002JD002499.

Adam, J. C., and D. P. Lettenmaier (2007), Application of new long-term precipitation, temperature, and reconstructed streamflow products to a streamflow trend attribution study in northern Eurasia, *J. Clim.*, in press.

Adam, J. C., E. A. Clark, D. P. Lettenmaier, and E. F. Wood (2006), Correction of global precipitation products for orographic effects, *J. Clim.*, *19*(1), 15–38.

Arctic Climate Impact Assessment (2005), *Arctic Climate Impact Assessment*, 1042 pp., Cambridge Univ. Press, New York.

Berezovskaya, S., D. Yang, and D. L. Kane (2004), Compatibility analysis of precipitation and runoff trends over the large Siberian watersheds, *Geophys. Res. Lett.*, *31*, L21502, doi:10.1029/2004GL021277.

Berezovskaya, S., D. Q. Yang, and L. Hinzman (2005), Long-term annual water balance analysis of the Lena River, *Global Planet. Change*, *48*(1–3), 84–95.

Bowling, L. C. (2002), Estimating the freshwater budget of high-latitude land areas, thesis, Univ. of Wash., Seattle.

Bowling, L. C., J. W. Pomeroy, and D. P. Lettenmaier (2004), Parameterization of blowing-snow sublimation in a macroscale hydrology model, *J. Hydrometeorol.*, *5*(5), 745–762.

Brodzik, M. J. (1997), EASE-Grid: A versatile set of equal-area projections and grids, Natl. Snow and Ice Data Cent., Boulder, Colo.

Cherkauer, K. A., and D. P. Lettenmaier (1999), Hydrologic effects of frozen soils in the upper Mississippi River basin, *J. Geophys. Res.*, *104*(D16), 19,599–19,610.

Cherkauer, K. A., and D. P. Lettenmaier (2003), Simulation of spatial variability in snow and frozen soil, *J. Geophys. Res.*, *108*(D22), 8858, doi:10.1029/2003JD003575.

Cherkauer, K. A., L. C. Bowling, and D. P. Lettenmaier (2003), Variable infiltration capacity cold land process model updates, *Global Planet. Change*, *38*(1–2), 151–159.

Dynesius, M., and C. Nilsson (1994), Fragmentation and flow regulation of river systems in the northern third of the world, *Science*, *266*(5186), 753–762.

Frauenfeld, O. W., T. Zhang, R. G. Barry, and D. Gilichinsky (2004), Interdecadal changes in seasonal freeze and thaw depths in Russia, *J. Geophys. Res.*, *109*, D05101, doi:10.1029/2003JD004245.

Georgievsky, V. Y., A. V. Ezhov, A. L. Shalygin, I. A. Shiklomanov, and A. I. Shiklomanov (1996), Assessment of the effect of possible climate changes on hydrological regime and water resources of rivers in the former USSR, *Russ. Meteorol. Hydrol.*, *11*, 66–74.

Groisman, P. Y. (2005), National Climatic Data Center Documentation for TD-9813, Daily and sub-daily precipitation for the Former USSR, 16 pp., Natl. Clim. Data Cent., Asheville, N. C.

Haddeland, I., D. P. Lettenmaier, and T. Skaugen (2006a), Effects of irrigation on the water and energy balances of the Colorado and Mekong river basins, *J. Hydrol.*, *324*(1–4), 210–223.

Haddeland, I., T. Skaugen, and D. P. Lettenmaier (2006b), Anthropogenic impacts on continental surface water fluxes, *Geophys. Res. Lett.*, *33*, L08406, doi:10.1029/2006GL026047.

Haddeland, I., T. Skaugen, and D. P. Lettenmaier (2007), Hydrologic effects of land and water management in North America and Asia: 1700–1992, *Hydrol. Earth Syst. Sci.*, *11*(2), 1035–1045.

Hamlet, A. F., and D. P. Lettenmaier (2005), Production of temporally consistent gridded precipitation and temperature fields for the continental United States, *J. Hydrometeorol.*, *6*(3), 330–336.

Hanasaki, N., S. Kanae, and T. Oki (2006), A reservoir operation scheme for global river routing models, *J. Hydrol.*, *327*(1–2), 22–41.

Hirsch, R. M., J. R. Slack, and R. A. Smith (1982), Techniques of trend analysis for monthly water-quality data, *Water Resour. Res.*, *18*(1), 107–121.

International Commission on Large Dams (2003), *World Register of Dams*, 340 pp., Paris.

Kalnay, E., et al. (1996), The NCEP/NCAR 40-year reanalysis project, *Bull. Am. Meteorol. Soc.*, *77*(3), 437–472.

Korobova, D. N. (1968), Optimization by dynamic programming of hydroelectric plant operation regime during initial filling period of multiannual regulation reservoir, *Hydrotech. Constr.*, *2*(5), 421–425.

Lammers, R. B., and A. I. Shiklomanov (2000), R-ArcticNet, a regional hydrographic data network for the pan-Arctic region, Water Syst. Anal. Group, Univ. of N. H., Durham. (Available at http://www.R-ArcticNET.sr.unh.edu)

Lammers, R. B., A. I. Shiklomanov, C. J. Vörösmarty, B. M. Fekete, and B. J. Peterson (2001), Assessment of contemporary Arctic river runoff based on observational discharge records, *J. Geophys. Res.*, *106*(D4), 3321–3334.

Liang, X., D. P. Lettenmaier, E. F. Wood, and S. J. Burges (1994), A simple hydrologically based model of land-surface water and energy fluxes for general-circulation models, *J. Geophys. Res.*, *99*(D7), 14,415–14,428.

Liebe, J., N. van de Giesen, and M. A. Andreini (2005), Estimation of small reservoir storage capacities in a semi-arid environment: A case study in the upper east region of Ghana, *Phys. Chem. Earth B*, *30*, 448–454.

Lohmann, D., R. Nolte-Holube, and E. Raschke (1996), A large-scale horizontal routing model to be coupled to land surface parameterization schemes, *Tellus, Ser. A*, *48*, 708–721.

Lohmann, D., E. Raschke, B. Nijssen, and D. P. Lettenmaier (1998), Regional scale hydrology: I. Formulation of the VIC-2L model coupled to a routing model, *Hydrol. Sci. J.*, *43*, 131–141.

Malik, L. K., N. Koronkevich, I. S. Zaitseva, and E. A. Barabanova (2000), Briefing paper on development of dams in the Russian Federation and other NIS countries, World Comm. on Dams, Cape Town, South Africa. (Available at http://www.dams.org/)

Mann, H. B. (1945), Nonparametric tests against trend, *Econometrica*, *13*, 245–259.

Maurer, E. P., A. W. Wood, J. C. Adam, D. P. Lettenmaier, and B. Nijssen (2002), A long-term hydrologically based dataset of land surface fluxes and states for the conterminous United States, *J. Clim.*, *15*(22), 3237–3251.

McClelland, J. W., R. M. Holmes, B. J. Peterson, and M. Stieglitz (2004), Increasing river discharge in the Eurasian Arctic: Consideration of dams, permafrost thaw, and fires as potential agents of change, *J. Geophys. Res.*, *109*, D18102, doi:10.1029/2004JD004583.

Mitchell, T. D., and D. Jones (2005), An improved method of constructing a database of monthly climate observations and associated high-resolution grids, *Int. J. Climatol.*, *25*(6), 693–712.

Nazarov, A. V. (1985), Experience in the operation of hydraulic structures and equipment of hydroelectric stations, *Power Technol. Eng.*, *19*(3), 154–161.

Nijssen, B., D. P. Lettenmaier, X. Liang, S. W. Wetzel, and E. F. Wood (1997), Streamflow simulation for continental-scale river basins, *Water Resour. Res.*, *33*(4), 711–724.

Nijssen, B., G. M. O'Donnell, A. F. Hamlet, and D. P. Lettenmaier (2001), Hydrologic sensitivity of global rivers to climate change, *Clim. Change*, *50*(1–2), 143–175.

Pavelsky, T. M., and L. C. Smith (2006), Intercomparison of four global precipitation data sets and their correlation with increased Eurasian river discharge to the Arctic Ocean, *J. Geophys. Res.*, *111*, D21112, doi:10.1029/2006JD007230.

Peterson, B. J., R. M. Holmes, J. W. McClelland, C. J. Vörösmarty, R. B. Lammers, A. I. Shiklomanov, I. A. Shiklomanov, and S. Rahmstorf (2002), Increasing river discharge to the Arctic Ocean, *Science*, *298*(5601), 2171–2173.

Platov, V. I. (1995), Hydropower of Russia: Prospects and urgent problems, *Hydrotech. Constr.*, *29*(8), 421–425.

Plishkin, G. A. (1979), Possible future hydrologic budget of the Ob' river basin, *Sov. Hydrol. Selec. Pap.*, *18*(4), 332–337.

Press, W. H., S. A. Teukolsky, W. T. Vetterling, and B. P. Flannery (1992), *Numerical Recipes in C*, 2nd ed., Cambridge Univ. Press, New York.

Rawlins, M. A., C. J. Willmott, A. Shiklomanov, E. Linder, S. Frolking, R. B. Lammers, and C. J. Vörösmarty (2006), Evaluation of trends in derived snowfall and rainfall across Eurasia and linkages with discharge to the Arctic Ocean, *Geophys. Res. Lett.*, *33*, L07403, doi:10.1029/2005GL025231.

Revenga, C., S. Murray, J. Abramovitz, and A. Hammond (1998), Watersheds of the world: Ecological value and vulnerability, World Resour. Inst. and Worldwatch Inst., Washington, D. C.

Savelieva, N. I., I. P. Semiletov, L. N. Vasilevskaya, and S. P. Pugach (2000), A climate shift in seasonal values of meteorological and hydrological parameters for northeastern Asia, *Prog. Oceanogr.*, *47*, 279–297.

Sheffield, J., A. D. Ziegler, E. F. Wood, and Y. Chen (2004), Correction of the high-latitude rain day anomaly in the NCEP/NCAR reanalysis for land surface hydrological modeling, *J. Clim.*, *17*, 3814–3828.

Shiklomanov, A. I., T. I. Yakovleva, R. B. Lammers, I. P. Karasev, C. J. Vörösmarty, and E. Linder (2006), Cold region river discharge uncertainty—Estimates from large Russian rivers, *J. Hydrol.*, *326*(1–4), 231–256.

Shiklomanov, I. A. (1978), Dynamics of anthropogenic changes in annual river runoff in the USSR, *Sov. Hydrol. Selec. Pap.*, *17*(1), 11–22.

Shiklomanov, I. A., and G. M. Veretennikova (1978), Effect of reservoirs on the annual runoff of rivers in the USSR, *Sov. Hydrol. Selec. Pap.*, *17*(1), 12–32.

Shiklomanov, I. A., A. I. Shiklomanov, R. B. Lammers, B. J. Peterson, and C. J. Vörösmarty (2000), The dynamics of river water inflow to the Arctic Ocean, in *The Freshwater Budget of the Arctic Ocean: Proceedings of the NATO Advanced Research Workshop*, edited by E. L. Lewis, pp. 281–296, Kluwer Acad., Norwell, Mass.

Snover, A. K., A. F. Hamlet, and D. P. Lettenmaier (2003), Climate-change scenario's for water planning studies—Pilot applications in the Pacific Northwest, *Bull. Am. Meteorol. Soc.*, *84*(11), 1513–1518.

Stafievskii, V. A., V. A. Bulatov, E. N. Reshetnikova, N. I. Stefanenko, L. S. Permyakova, and A. P. Epifanov (2003), State of the dam of the Sayano-Shushenskaya hydropower plant in the last stage of reconditioning of the pressure-face concrete and contact zone of the rock bed, *Power Technol. Eng.*, *37*(6), 331–337.

Storck, P., and D. P. Lettenmaier (1999), Predicting the effect of a forest canopy on ground snow accumulation and ablation in maritime climate, in *Proceedings of the 67th Snow Conference*, edited by C. Troendle, pp. 1–12, Colo. State Univ., Fort Collins.

Su, F., J. C. Adam, L. C. Bowling, and D. P. Lettenmaier (2005), Streamflow simulations of the terrestrial Arctic domain, *J. Geophys. Res.*, *110*, D08112, doi:10.1029/2004JD005518.

Sun, S., and X. Zhang (2004), Effect of the lower boundary position of the Fourier equation on the soil energy balance, *Adv. Atmos. Sci.*, *21*(6), 868–878.

Taylor, J. R. (1997), *An Introduction to Error Analysis: The Study of Uncertainties in Physical Measurements*, 2nd ed., 327 pp., Univ. Sci. Books, Sausalito, Calif.

Vörösmarty, C. J., and D. Sahagian (2000), Anthropogenic disturbance of the terrestrial water cycle, *Bioscience*, *50*(9), 753–765.

Vörösmarty, C. J., K. P. Sharma, B. M. Fekete, A. H. Copeland, J. Holden, J. Marble, and J. A. Lough (1997), The storage and aging of continental runoff in large reservoir systems of the world, *Ambio*, *26*(4), 210–219.

Vrugt, J. A., H. V. Gupta, W. Bouten, and S. Sorooshian (2003), A Shuffled Complex Evolution Metropolis algorithm for optimization and uncertainty assessment of hydrologic model parameters, *Water Resour. Res.*, *39*(8), 1201, doi:10.1029/2002WR001642.

Vyruchalkina, T. Y. (2004), Lake Baikal and the Angara River before and after the construction of reservoirs, *Water Resour.*, *31*(4), 526–532.

Willmott, C. J., and K. Matsuura (2005), Arctic land-surface precipitation: 1930–2004 gridded monthly time series (V. 1.03), Cent. for Clim. Res., Univ. of Del., Newark.

Wood, A. W., L. R. Leung, V. Sridhar, and D. P. Lettenmaier (2004), Hydrologic implications of dynamical and statistical approaches to downscaling climate model outputs, *Clim. Change*, *62*(1–3), 189–216.

Wu, P., R. Wood, and P. Stott (2005), Human influence on increasing Arctic river discharges, *Geophys. Res. Lett.*, *32*, L02703, doi:10.1029/2004GL021570.

Yang, D., D. L. Kane, L. D. Hinzman, X. Zhang, T. Zhang, and H. Ye (2002), Siberian Lena River hydrologic regime and recent change, *J. Geophys. Res.*, *107*(D23), 4694, doi:10.1029/2002JD002542.

Yang, D., D. Robinson, Y. Zhao, T. Estilow, and B. Ye (2003), Streamflow response to seasonal snow cover extent changes in large Siberian watersheds, *J. Geophys. Res.*, *108*(D18), 4578, doi:10.1029/2002JD003149.

Yang, D. Q., B. S. Ye, and D. L. Kane (2004a), Streamflow changes over Siberian Yenisei River Basin, *J. Hydrol.*, *296*(1–4), 59–80.

Yang, D. Q., B. S. Ye, and A. Shiklomanov (2004b), Discharge characteristics and changes over the Ob River watershed in Siberia, *J. Hydrometeorol.*, *5*(4), 595–610.

Ye, B., D. Yang, and D. L. Kane (2003), Changes in Lena River streamflow hydrology: Human impacts versus natural variations, *Water Resour. Res.*, *39*(7), 1200, doi:10.1029/2003WR001991.

Ye, H., D. Q. Yang, T. Zhang, X. Zhang, S. Ladochy, and M. Ellison (2004), The impact of climatic conditions on seasonal river discharges in Siberia, *J. Hydrometeorol.*, *5*, 286–295.

J. C. Adam, D. P. Lettenmaier, and F. Su, Department of Civil and Environmental Engineering, University of Washington, Box 352700, Seattle, WA 98195-2700, USA. (jadam@u.washington.edu; dennisl@u.washington.edu; fgsu@hydro.washington.edu)

I. Haddeland, Norwegian Water Resources and Energy Directorate, Box 5091, N-0301 Oslo, Norway. (ingjerd.haddeland@nve.no)